

February 2026

# Hard thermal contributions to phase transition observables at NNLO

Fabio Bernardo<sup>ab,\*</sup> Mikael Chala<sup>b,†</sup> Luis Gil<sup>b,‡</sup> and Philipp Schicho<sup>ab,§</sup>

<sup>a</sup>*Département de Physique Théorique, Université de Genève,  
24 quai Ernest Ansermet, CH-1211 Genève 4, Switzerland*

<sup>b</sup>*Departamento de Física Teórica y del Cosmos, Universidad de Granada,  
Campus de Fuentenueva, E-18071 Granada, Spain*

## Abstract

To construct the high-temperature effective field theory of gauge-Higgs models up to  $\mathcal{O}(g^6)$  in the gauge coupling, we integrate out hard modes to three-loop level and use the next-to-next-to-leading order effective potential. For the Abelian Higgs model, we quantify the impact of both higher-dimensional operators and higher-loop corrections on thermodynamic parameters relevant for gravitational-wave observables, finding that one-loop dimension-six effects typically dominate over two- and three-loop corrections to super-renormalizable parameters for the strongest transitions. We derive the three-loop scalar and Debye masses for the U(1) and SU( $N$ ) gauge-Higgs models, as well as the two-loop quartic couplings for the Abelian case, show gauge independence of physical parameters, and demonstrate that no new master integrals are required for the matching, while consistency of 4d and 3d renormalizability points to previously missing contributions in these master integrals.

---

\*fabio.bernardo@unige.ch

†mikael.chala@ugr.es

‡lgil@ugr.es

§philipp.schicho@unige.ch

## Contents

<b>1</b>	<b>Introduction</b>	<b>2</b>
<b>2</b>	<b>Setup</b>	<b>3</b>
<b>3</b>	<b>High-temperature effective field theory</b>	<b>4</b>
3.1	Effective theory at the soft scale	5
<b>4</b>	<b>Higher-order corrections to equilibrium thermodynamics</b>	<b>10</b>
4.1	Comparing higher-dimensional operators against loop corrections	14
<b>5</b>	<b>Outlook</b>	<b>17</b>
<b>A</b>	<b>Renormalization group equations</b>	<b>18</b>
<b>B</b>	<b>Master integrals</b>	<b>19</b>
<b>C</b>	<b>Details of dimensional reduction</b>	<b>21</b>
C.1	Three-loop thermal masses in the Abelian Higgs model	27
C.2	Three-loop thermal masses in the $SU(N) +$ fundamental scalar model	29
C.3	On the mismatch in the master integral $\mathcal{I}_{31111-2}$	33

## 1. Introduction

The potential future observation of a stochastic gravitational wave (GW) background of cosmological origin has opened the door to entirely new avenues in high energy physics research. In particular, one type of source that has drawn a lot of interest in recent years are strong first-order phase transitions (PTs) associated to symmetry breaking in the early universe [1–6]. The reason is that the Standard Model (SM) does not predict any PT neither in the electroweak [7–9] nor in the QCD sectors [10–18], so observing a GW background compatible with such a transition would be an undeniable proof of new physics.

Studying these thermally-induced transitions typically relies on effective field theory (EFT) methods, such as high-temperature dimensional reduction, which systematically integrates out the effect from heavy thermal excitations [19] in favor of a three-dimensional EFT (3d EFT) for the infrared bosonic modes. The systematics of this EFT framework were clarified long ago [20, 21], and it has since become a cornerstone in the study of physics of thermal equilibrium. In this construction, higher-order effects from heavy modes are encoded in a tower of local operators that arise in a perturbative expansion in  $m_{\text{eff}}/(\pi T)$ , where  $m_{\text{eff}}$  is the mass of the field driving the transition and  $\pi T$  is the heavy thermal scale that is integrated out.

Most existing studies that explore PTs within dimensional reduction [22–62] focus on leading-order contributions in the 3d EFT while omitting operators beyond the super-renormalizable level. While this approximation suffices for weaker PTs driven by thermal loop effects, recent studies [46, 53, 54, 56, 61, 62] provide increasing evidence that an accurate description of moderately strong PTs requires including marginal operators, such as dimension-6 terms.<sup>1</sup> Their inclusion turns out to be crucial to reduce the large uncertainties that populate nucleation computations for strong transitions [27], namely gauge and scale dependence, which become relevant if one truncates the EFT expansion at low orders [53, 54]. In the limit of very strong PTs, the high-temperature expansion breaks altogether and alternative approaches have recently been suggested [59]. For weaker transitions, the perturbative series must be reorganized until non-perturbative effects become relevant. In this regime, thermal loop corrections are dominant. In the intermediate regime, higher-order operators and loop corrections within the 3d EFT framework can bridge the gap between these two limiting cases, while simultaneously scrutinizing the validity of broad-temperature approaches.

In this work, we build upon this direction by providing a thorough analysis of the high-temperature limit of the Abelian Higgs model at  $\mathcal{O}(g^6)$  in the gauge coupling constant. Employing the usual power counting [38, 63], this implies the computation of three-loop matching contributions to the masses, two-loop contributions to couplings, and one-loop

---

<sup>1</sup>Henceforth, unless otherwise stated, we use four-dimensional (4d) units when discussing energy dimensions, even though these operators live in 3d Euclidean space.

contributions to dimension-6 operators in the 3d EFT. The Abelian Higgs model is the simplest model that captures the essential features of more complex gauge–Higgs theories, and serves as a playground to explore the difficulties and consequences of such high-order computations. In particular, extending [53, 56], our main goals are threefold:

- (a) to prove the cancellation of gauge dependence order by order in loops,
- (b) to show the convergence of 3d parameters, by inspecting their increasingly small renormalization scale dependence at higher orders, and
- (c) to quantify the relevance of higher-dimensional operators in strong PTs and compare it to the contribution of the three-loop matching.

As a byproduct, we recover a series of integration-by-part relations [64] for three-loop bosonic sum-integrals and show that no new master integrals appear in the computation of the thermal scalar masses in generic  $SU(N)$  gauge theories with a fundamental scalar.

The article is organized as follows. Section 2 introduces the Abelian Higgs model. The details of its dimensional reduction are presented in sec. 3. Section 4 describes the computation of the critical parameters and assesses the contribution from different orders in perturbation theory. Section 5 summarizes our results and outlines future lines of work. Technical details of our computations are relegated to appendices A, B and C.

## 2. Setup

We consider the high-temperature limit of a  $U(1)$  gauge theory coupled to a complex fundamental scalar  $\phi$  with unit charge. In four-dimensional (4d) Euclidean space, the theory is described by the Lagrangian

$$\mathcal{L}_{4d} = \frac{1}{4}F_{\mu\nu}F_{\mu\nu} + (D_\mu\phi)^\dagger(D_\mu\phi) + \mu^2\phi^\dagger\phi + \lambda(\phi^\dagger\phi)^2 + \mathcal{L}_{GF}, \quad (2.1)$$

where  $F_{\mu\nu} = \partial_\mu B_\nu - \partial_\nu B_\mu$  is the field strength tensor and the covariant derivative is defined as  $D_\mu = \partial_\mu - igB_\mu$ , with  $g$  being the gauge coupling. The  $R_\xi$  gauge-fixing term reads

$$\mathcal{L}_{GF} = \frac{1}{2\xi}(\partial_\mu B_\mu)^2. \quad (2.2)$$

Far from a toy model, this theory plays a significant role in the study of dark-sector PTs that are decoupled from the SM [65–69]. Moreover, it is closely related to condensed matter physics, where its 3d counterpart provides a mean-field description of superconductivity [70–72]. More recently, the classically conformal Abelian Higgs model has been used to study primordial black hole formation from supercooled PTs [73], though their predicted abundances remain limited by the constraints of the formation mechanism [74, 75].

### 3. High-temperature effective field theory

One major challenge in finite-temperature computations is the emergence of a hierarchy of dynamically generated scales due to in-medium effects. These scales are defined relative to the hard scale  $\pi T$ , which sets the typical energy of on-shell particles at high temperatures, and in a gauge theory they read [76]

$$\underbrace{\pi T}_{\text{hard scale}} \gg \underbrace{gT}_{\text{soft scale}} \gg \underbrace{g^{3/2}T}_{\text{softer scale}} \gg \underbrace{g^2T}_{\text{ultrasoft scale}} , \quad (3.1)$$

where  $g$  is the largest gauge coupling, which we use as the power counting parameter.<sup>2</sup>

The first scale is that of the heavy Matsubara modes, whose masses are of  $\mathcal{O}(\pi T)$  [19]. The second is associated with the screening of bosonic zero modes, which induces a Debye mass of  $\mathcal{O}(gT)$  for the temporal component of gauge bosons. The third corresponds to the thermal effective mass of the scalar driving the transition, which can become parametrically smaller than the soft scale near the critical temperature. Finally, the ultrasoft scale corresponds to non-perturbative contributions from spatial gauge bosons in the deep infrared [77].

This plethora of hierarchies is problematic, since it leads to the appearance of large logarithms in perturbative computations. One way to systematically handle them is to use finite-temperature EFT techniques [10, 76, 78]. This framework consists in building a tower of effective theories by successively integrating out heavy degrees of freedom with respect to each scale, through a process called *matching*. With this, at lower scales the resulting effective Wilson coefficients are renormalization-group (RG) improved, ensuring the resummation of large logarithms.

In going from the hard to the soft scale, one performs *dimensional reduction* (DR), constructing a static 3d EFT for bosonic zero modes. The EFT parameters encode all temperature dependence. At scales below the hard scale, the matching between different 3d theories follows the standard vacuum procedure and is temperature-independent. Schematically, there exist two alternative constructions [78],

$$\mathcal{L}_{4d} \xrightarrow{\text{DR}} \mathcal{L}_{\text{soft}} \mapsto \mathcal{L}_{\text{softer}} \mapsto V_{\text{eff}} , \quad (\text{DR-A})$$

$$\mathcal{L}_{4d} \xrightarrow{\text{DR}} \mathcal{L}_{\text{soft}} \mapsto V_{\text{eff}} , \quad (\text{DR-B})$$

where the final mapping indicates that the effective potential  $V_{\text{eff}}$  is computed at the lowest energy scale in each respective approach.

As demonstrated in [53], the approach in (DR-A) becomes unreliable in the regime of strong PTs, where nucleation takes place already at the soft scale. Indeed, the softer EFT Lagrangian can be written as an expansion in operators of increasing dimension,

$$\mathcal{L}_{\text{softer}} \supset \text{const.} \times \frac{\Lambda_{\text{soft}}^3}{4\pi} \left( \frac{D_i}{\Lambda_{\text{soft}}} \right)^m \left( \frac{g_3 \phi}{\Lambda_{\text{soft}}} \right)^n , \quad (3.2)$$

---

<sup>2</sup>Following [53], we adopt the power counting  $\mu^2/T^2 \sim \lambda \sim g^2$  for 4d parameters.

where  $\Lambda_{\text{soft}} \sim gT$  is the soft scale,  $g_3$  is the effective gauge coupling,  $D_i$  denotes the gauge covariant derivative, and  $\phi$  is the scalar driving the transition. For strong PTs, the scalar vacuum expectation value (vev) in the broken phase typically becomes much larger than  $\Lambda_{\text{soft}}/g_3$ , leading to a breakdown of the operator expansion, which invalidates the softer scale description.

The dimensional reduction of the Abelian Higgs model, including higher-dimensional operators, was carried out in [53]. There, the matching was performed at two-loop level (or  $\mathcal{O}(g^4)$ ) for dimension-two operators, namely for the scalar and Debye masses; and at one-loop level (or  $\mathcal{O}(g^4)$ ) for dimension-four operators as well as for higher-dimensional operators, which first appear at  $\mathcal{O}(g^6)$ . While gauge dependence was shown to cancel consistently for dimension-6 operators upon redefinition onto a physical basis, a residual gauge-dependent contribution was found at  $\mathcal{O}(g^6)$  in the scalar mass; see eq. (B.68) in [53].

As we shall see, the gauge-dependent contribution arising from the three-loop matching of the mass parameters, which enters at  $\mathcal{O}(g^6)$ , precisely cancels this residual gauge dependence. As a result, the 3d EFT is fully gauge independent up to  $\mathcal{O}(g^6)$ . Furthermore, our analysis provides new results for the two-loop matching of the quartic operators up to  $\mathcal{O}(g^6)$ .

### 3.1. Effective theory at the soft scale

In the soft-scale 3d EFT Lagrangian (**DR-B**),

$$\begin{aligned} \mathcal{L}_{\text{soft}} = & \frac{1}{4} F_{ij} F_{ij} + (D_i \phi)^\dagger (D_i \phi) + \mu_3^2 (\phi^\dagger \phi) + \frac{1}{2} (\partial_i B_0)^2 + \frac{1}{2} m_{\text{D}}^2 (B_0)^2 \\ & + \lambda_3 (\phi^\dagger \phi)^2 + h_3 (\phi^\dagger \phi) (B_0)^2 + \kappa_3 (B_0)^4 + \frac{1}{2\xi} (\partial_\mu B_\mu)^2 + \mathcal{L}_{\text{soft}}^{(6)}, \end{aligned} \quad (3.3)$$

with a little abuse of notation, we have introduced the zero modes of the scalar,  $\phi$ , the spatial gauge field  $B_i$ , and the temporal gauge field  $B_0$ , which have (3d) mass dimension  $[\phi] = [B_i] = [B_0] = 1/2$  when normalized canonically. The 3d covariant derivative is given by  $D_i = \partial_i - i g_3 B_i$ , with effective gauge coupling  $g_3$ . Finally,  $\mathcal{L}_{\text{soft}}^{(6)}$  contains a basis of dimension-6 operators.

In this section, we focus on the effective scalar mass  $\mu_3^2$  and Debye mass  $m_{\text{D}}^2$ , since these are the only parameters that must be computed at three-loop order to achieve  $\mathcal{O}(g^6)$  accuracy. The matching relations for the static screening masses  $\Pi(k_0 = 0, \mathbf{k} \rightarrow 0)$  of the scalar field and the temporal gauge field are obtained by matching the poles of the corresponding static propagators [64], *viz.*

$$\begin{aligned} \mu_3^2 = & \mu^2 + \Pi_{\phi^\dagger \phi}^{1\ell} + \Pi_{\phi^\dagger \phi}^{2\ell} - \left( \mu^2 + \Pi_{\phi^\dagger \phi}^{1\ell} + \Pi_{\phi^\dagger \phi}^{2\ell} \right) \Pi_{\phi^\dagger \phi}^{1\ell, (1)} \\ & + \left( \mu^2 + \Pi_{\phi^\dagger \phi}^{1\ell} \right) \left[ \left( \Pi_{\phi^\dagger \phi}^{1\ell, (1)} \right)^2 + \left( \mu^2 + \Pi_{\phi^\dagger \phi}^{1\ell} \right) \Pi_{\phi^\dagger \phi}^{1\ell, (2)} - \Pi_{\phi^\dagger \phi}^{2\ell, (1)} \right] + \Pi_{\phi^\dagger \phi}^{3\ell} - \delta \mu_3^2, \end{aligned} \quad (3.4)$$

$$m_{\text{D}}^2 = \Pi_{B_0 B_0}^{1\ell} + \Pi_{B_0 B_0}^{2\ell} - \left( \Pi_{B_0 B_0}^{1\ell} + \Pi_{B_0 B_0}^{2\ell} \right) \Pi_{B_0 B_0}^{1\ell, (1)}$$

$$\begin{aligned}
\phi \circledcirc (3\ell) &= \text{ (246 diagrams)} \\
&+ \text{ (246 diagrams)} \\
B_\mu \circledcirc (3\ell) &= \text{ (240 diagrams)} \\
&+ \text{ (240 diagrams)}
\end{aligned}$$

Figure 1: Three-loop contributions to the bare two-point functions in the Abelian Higgs model at the soft scale. Dashed directed lines denote scalars ( $\phi$ ) and wiggly lines denote gauge fields ( $B_\mu$ ).

$$\begin{aligned}
\circledcirc (2\ell) B_\mu &= \text{ (560 diagrams)} \\
\circledcirc (2\ell) \phi &= \text{ (525 diagrams)} \\
\circledcirc (2\ell) &= \text{ (401 diagrams)}
\end{aligned}$$

Figure 2: Two-loop contributions to the bare four-point functions in the Abelian Higgs model at the soft scale including all possible permutations of external legs. Dashed directed lines denote scalars ( $\phi$ ) and wiggly lines denote gauge fields ( $B_\mu$ ).

$$+ \Pi_{B_0 B_0}^{1\ell} \left[ (\Pi_{B_0 B_0}^{1\ell, (1)})^2 + \Pi_{B_0 B_0}^{1\ell} \Pi_{B_0 B_0}^{1\ell, (2)} - \Pi_{B_0 B_0}^{2\ell, (1)} \right] + \Pi_{B_0 B_0}^{3\ell} - \delta m_D^2, \quad (3.5)$$

where  $n\ell = 1\ell, \dots, 3\ell$  indicates the different loop levels,  $\Pi^{n\ell}$  is the  $n$ -loop renormalized correlator, and the  $\Pi^{(n)} = \Pi^{(1)}, \dots, \Pi^{(2)}$  superscripts indicate the order of momentum derivatives. Finally,  $\delta\mu_3^2$  and  $\delta m_D^2$  are the corresponding mass counterterms in the 3d EFT; see eqs. (C.29) and (C.30).

As seen from eqs. (3.4) and (3.5), to reach  $\mathcal{O}(g^6)$  accuracy, self-energies are required up to three-loop order, including higher-order momentum derivatives of the one- and two-loop contributions. The diagrams for the bare three-loop correlators  $\Pi_{\phi^\dagger \phi}^{3\ell, (B)}$  and  $\Pi_{B_0 B_0}^{3\ell, (B)}$  are listed in fig. 1 while their corresponding analytic expressions are collected in appendix C. In addition to the three-loop contributions to the scalar and Debye masses, two-loop contributions to the quartic couplings  $\lambda_3$ ,  $h_3$ , and  $\kappa_3$  are required for  $\mathcal{O}(g^6)$  accuracy. These are obtained by matching the corresponding four-point functions at zero external momenta. The two-loop diagrams for the bare quartic correlators are shown in fig. 2, and their expressions are also

collected in appendix C.

The masses are renormalized upon the introduction of the renormalized 4d parameters in eqs. (3.4) and (3.5); see appendix A. We do this perturbatively as follows. Let  $L = 3$  be the loop order of the computation, and let  $\Pi^{n\ell,(B)} = f(c_i^{(B)})$  be the bare  $n$ -loop ( $n \leq L$ ) piece of a given correlator, which is an analytic function  $f$  of the bare parameters  $c_i^{(B)}$ . The corresponding renormalized parameters can be written as  $c_i = c_i^{(B)} + \sum_{k=1}^L \delta c_i^{k\ell}$ , where  $\delta c_i^{k\ell}$  are the  $k$ -loop associated counterterms. Now, we obtain the renormalized masses upon replacing  $c_i^{(B)} \rightarrow c_i - \sum_{k=1}^L \delta c_i^{k\ell}$  perturbatively in loops in each of the  $n$ -loop correlator pieces, up to  $L$ -loop order. This well-known perturbative renormalization procedure naturally mixes lower-loop correlators with counterterm insertions and higher-loop correlators without counterterm insertions. Finally, we subtract the 3d mass counterterms to remove all leftover divergences from the hard region expansion of the 4d and 3d correlators, which yields a fully renormalized 3d effective mass.

The expressions for the (renormalized) scalar and Debye masses, up to three-loop level and  $\mathcal{O}(g^6)$  accuracy, read

$$\begin{aligned}
\mu_3^2 = & [\mu^2]_{\text{tree level}} + T^2 \left[ \frac{g^2}{4} + \frac{\lambda}{3} \right]_{\text{1 loop}} \\
& + \frac{T^2}{(4\pi)^2} \left[ g^4 \left( -\frac{13}{12}L_b + 3L_{3d} + \frac{25}{9} \right) + g^2 \lambda \left( 2L_b - 4L_{3d} - \frac{10}{3} \right) \right. \\
& \quad \left. + \lambda^2 \left( -\frac{10}{3}L_b + 4L_{3d} + 4 \right) + \frac{\mu^2}{T^2} (3g^2 - 4\lambda) L_b \right]_{\text{2 loop}} \\
& + \frac{T^2}{(4\pi)^4} \left[ g^4 \lambda \left( 32L_{3d} - \frac{140}{3}L_b L_{3d} + \frac{47}{3}L_b^2 - \frac{544}{9}L_b + C_1 \right) \right. \\
& \quad \left. + \lambda^3 \left( -80L_b L_{3d} + \frac{100}{3}L_b^2 - 40L_b + C_2 \right) \right. \\
& \quad \left. + g^6 \left( 10L_b L_{3d} - \frac{16}{3}L_{3d} - \frac{95}{36}L_b^2 + \frac{487 - 45X}{27}L_b + C_3 \right) \right. \\
& \quad \left. + g^2 \lambda^2 \left( 88L_b L_{3d} - 30L_b^2 + \frac{188}{3}L_b + C_4 \right) \right. \\
& \quad \left. + g^4 \frac{\mu^2}{T^2} \left( 10L_b^2 - \frac{43}{3}L_b - \frac{7}{36}(12\zeta_3 + 25) \right) \right. \\
& \quad \left. + g^2 \lambda \frac{\mu^2}{T^2} \left( -24L_b^2 - 32L_b + \frac{16}{9}(\zeta_3 - 27) \right) \right. \\
& \quad \left. + \lambda^2 \frac{\mu^2}{T^2} \left( 28L_b^2 + 20L_b + \frac{1}{3}(16\zeta_3 + 89) \right) \right. \\
& \quad \left. - g^2 \frac{\mu^4}{T^4} \left( \frac{10\zeta_3}{3} \right) + \lambda \frac{\mu^4}{T^4} (8\zeta_3) - \frac{2 + 5X}{9\epsilon} g^6 T^2 \right]_{\text{3 loop}} + \mathcal{O}(g^8), \tag{3.6}
\end{aligned}$$

$$\begin{aligned}
m_{\text{D}}^2 = & T^2 \left[ \frac{g^2}{3} \right]_{1 \text{ loop}} + \frac{T^2}{(4\pi)^2} \left[ -g^4 \frac{L_b - 7}{9} + \frac{4}{3} g^2 \lambda + 4 \frac{\mu^2}{T^2} g^2 \right]_{2 \text{ loop}} \\
& + \frac{T^2}{(4\pi)^4} \left[ g^6 \left( \frac{1}{27} L_b^2 - \frac{158}{27} L_b + \frac{8}{3} L_{3d} + \frac{1}{270} (3220 - 57\zeta_3) \right) \right. \\
& \quad + g^4 \lambda \left( \frac{68}{9} L_b + 16 L_{3d} - \frac{8(\zeta_3 + 34)}{9} \right) - g^2 \lambda^2 \left( \frac{40}{3} L_b + \frac{4}{9} (2\zeta_3 - 21) \right) \\
& \quad + g^4 \frac{\mu^2}{T^2} \left( \frac{32}{3} L_b - \frac{8}{3} (\zeta_3 - 11) \right) \\
& \quad \left. - g^2 \lambda \frac{\mu^2}{T^2} \left( 16 L_b + \frac{16\zeta_3}{3} \right) - 8\zeta_3 g^2 \frac{\mu^4}{T^4} \right]_{3 \text{ loop}} + \mathcal{O}(g^8). \tag{3.7}
\end{aligned}$$

In analogy to [64], we expressed the results in terms of

$$L_b \equiv 2 \ln \frac{\bar{\Lambda} e^{\gamma_E}}{4\pi T}, \quad L_{3d} \equiv \ln \frac{\bar{\Lambda}_{3d}^2 e^{Z_1}}{4\pi T^2}, \tag{3.8}$$

where  $\bar{\Lambda}$  is the 4d  $\overline{\text{MS}}$  matching scale,  $\bar{\Lambda}_{3d}$  is the 3d EFT running scale, and we abbreviate derivatives of the Riemann  $\zeta$ -function  $\zeta_s \equiv \zeta(s)$  by  $Z_s^{(n)} = \zeta_{-s}^{(n)}/\zeta_{-s}$ . Finally,  $C_1, \dots, C_4$  are constants coming from the three-loop integrals that have been numerically evaluated (cf. appendix B),

$$\begin{aligned}
C_1 &\simeq -205.26752454(7), & C_2 &\simeq -562.620736703785(16), \\
C_3 &\simeq -23.2884964(6) + \frac{5}{3} \gamma_E X, & C_4 &\simeq 449.912927014132(4). \tag{3.9}
\end{aligned}$$

Here, we defined  $X$  to parametrize a potential mismatch in the  $\mathcal{O}(\epsilon^{-1}, \epsilon^0)$  parts of the master integral (B.8) of the form  $\mathcal{I}_{31111-2} \rightarrow \mathcal{I}_{31111-2} + \delta\mathcal{I}_{31111-2}$ , where

$$\delta\mathcal{I}_{31111-2} \equiv -\frac{T^2}{(4\pi)^4} \left( \frac{1}{4\pi T^2} \right)^{3\epsilon} \frac{5X}{36\epsilon}. \tag{3.10}$$

This mismatch causes the residual  $1/\epsilon$  pole in the renormalized 3d scalar mass shown in eq. (3.6). As discussed in appendix C.3, the same issue arises in the  $\text{SU}(N)$  case. Setting  $X = -2/5$  restores finiteness of the scalar masses in both theories.

As shown in eq. (3.6), the gauge dependence cancels completely once the three-loop contribution is included. The corresponding plots for expressions (3.7) and (3.6) as functions of the temperature are shown in the upper panels of fig. 3. Using the following benchmark (BM) values of the  $\overline{\text{MS}}$  parameters at the input scale  $\bar{\Lambda}_{\text{in}}$ ,

$$\bar{\Lambda}_{\text{in}} = 1 \text{ GeV}, \quad g(\bar{\Lambda}_{\text{in}}) = 1, \quad \lambda(\bar{\Lambda}_{\text{in}}) = 0.1, \quad \mu^2(\bar{\Lambda}_{\text{in}}) = -0.01 \text{ GeV}^2, \tag{BM1}$$

the 4d couplings are evolved to the 4d matching scale  $\bar{\Lambda}$  using two-loop RG equations given in eq. (A.4), while varying  $\bar{\Lambda}$  in the range  $\bar{\Lambda} \in [2^{-3}, 2^3] \pi T$  to illustrate the reduced dependence on the matching scale at higher orders in the EFT matching. The 3d renormalization

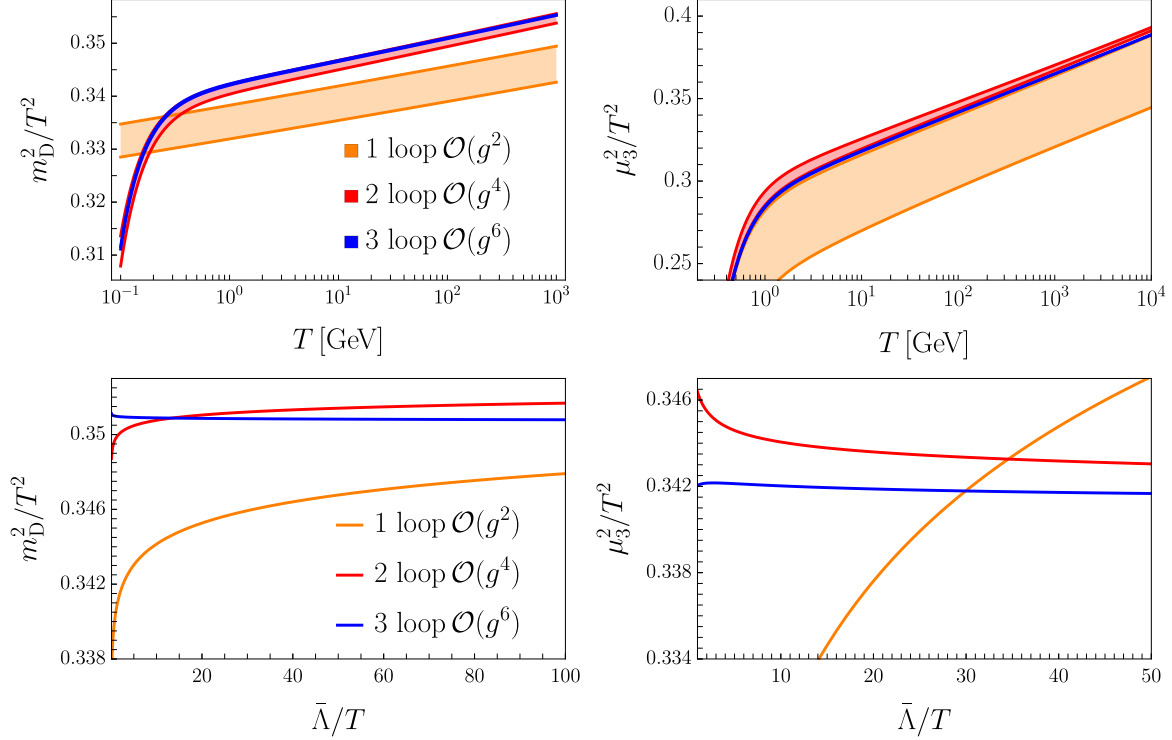


Figure 3: Debye (left panels) and scalar (right panels) masses as functions of temperature (top row) and matching scale  $\bar{\Lambda}$  at  $T = 100$  GeV (bottom row). The 4d couplings are fixed at (BM1). The 3d renormalization scale is set to the optimized value  $\bar{\Lambda}_{3d,\text{opt}} = 2.85 T$  [64, 79, 80], and we assume  $X = 0$ . Setting  $X$  to slightly different values (for instance,  $X = -2/5$ ) leads to only imperceptible deviations in the results. In the upper panels, the matching scale is varied in the range  $\bar{\Lambda} \in [2^{-3}, 2^3] \pi T$ . The  $n$ -loop curves show the  $n$ -loop matching results for the Debye and scalar masses, with the 4d parameters evolved using two-loop running (A.4). The plots illustrate that the dependence on the matching scale is further suppressed at higher orders when two-loop running and three-loop matching contributions are included.

scale is set to the optimized value  $\bar{\Lambda}_{3d,\text{opt}} = 2.85 T$ , determined via the principle of minimal sensitivity [79], following the approach used for the QCD Debye mass [64, 80].

As a crosscheck, we verify that the 3d mass parameters in eqs. (3.6) and (3.7) are independent of the matching scale  $\bar{\Lambda}$  order by order in  $g$ . Using the running of the 4d couplings  $g$ ,  $\lambda$ , and  $\mu^2$  given in eq. (A.4), we find

$$\partial_t \mu_3^2 = -\frac{2+5X}{384\pi^4} g^6 T^2 + \mathcal{O}(g^8), \quad \partial_t m_D^2 = \mathcal{O}(g^8), \quad (3.11)$$

where  $t \equiv \ln \bar{\Lambda}$ . Here, the mismatch in the master integral introduces some residual scale dependence at  $\mathcal{O}(g^6)$  in  $\mu_3^2$ . Again, setting  $X = -2/5$  consistently pushes the dependence on

$\bar{\Lambda}$  to higher orders, which further points at a potential error in the  $\mathcal{O}(\epsilon^{-1}, \epsilon^0)$  parts of the master integral (B.8) from [81]. We show the reduced dependence of the 3d masses on the matching scale  $\bar{\Lambda}$  in the lower panels of fig. 3.

The matching procedure for the 3d masses as outlined in eqs. (3.4) and (3.5), is consistent with performing the EFT matching in an off-shell operator basis and subsequently carrying out field redefinitions to eliminate redundancies and extract the effective parameters in an on-shell operator basis as shown in [82], and applied at finite temperature in [53, 54, 56]. To determine the rest of the effective parameters besides the thermal masses, we follow the off-shell matching procedure. Further details are provided in appendix C.

Having determined the full  $\mathcal{O}(g^6)$  soft-scale EFT, we now aim to determine the soft-scale effective potential to compute all critical parameters.

#### 4. Higher-order corrections to equilibrium thermodynamics

We organize the perturbative expansion of the effective potential following the power counting presented in [63]. Higher-dimensional operators are left unassigned to a specific perturbative order, but are assumed to be subleading relative to the leading-order (LO) effective potential, *viz.*<sup>3</sup>

$$\frac{V_{\text{eff}}}{T^3} \sim \left[ \frac{g^3}{\pi} \right]_{\text{LO}} + \left[ \frac{g^4}{\pi^2} \right]_{\text{NLO}} + \left[ \frac{g^{9/2}}{\pi^{5/2}} \right]_{\text{N}^2\text{LO}} + \left[ \frac{g^6}{\pi^4} \right]_{\text{dim6}} + \left[ \mathcal{O}\left(\frac{g^5}{\pi^3}\right) \right]_{\text{N}^3\text{LO}}, \quad (4.1)$$

where we neglect  $\text{N}^3\text{LO}$  super-renormalizable contributions to  $V_{\text{eff}}$ . Although the dimension-6 term may appear subleading compared to the neglected  $\text{N}^3\text{LO}$  contribution, its  $g^6$  scaling reflects the parametric size of the corresponding Wilson coefficients rather than the operator itself, which involves higher powers of fields than super-renormalizable operators. We therefore remain agnostic about its numerical importance.

The terms of eq. (4.1) originate from

$$\begin{aligned} V_{\text{eff}}^{\text{LO}} &\sim g^3 && \text{tree-level scalar and one-loop vector and temporal scalar ,} \\ V_{\text{eff}}^{\text{NLO}} &\sim g^4 && \text{two-loop vector and temporal scalar ,} \\ V_{\text{eff}}^{\text{N}^2\text{LO}} &\sim g^{\frac{9}{2}} && \text{one-loop scalar ,} \\ V_{\text{eff}}^{\text{dim6}} &\sim g^6 && \text{tree-level higher-dimensional operators .} \end{aligned}$$

Our choice to include higher-dimensional operators as a correction to the LO effective potential is not arbitrary. While one cannot, in general, assign an all-encompassing power

---

<sup>3</sup>Henceforth, we assume that  $\lambda \sim g^3$  [83], which is more appropriate in the region of the 4d parameter space that we explore. Upon this change, our matching equations are still correct up to  $\mathcal{O}(g^6)$ , but terms involving more powers of  $\lambda$  will be in practice further suppressed.

counting for higher-dimensional operators in this context, the validity of the high-temperature expansion does impose strict constraints [84].

For a general  $N$ -dimensional scalar multiplet  $\phi$  in the broken phase, we shift the field by a real background  $v$  defined by  $\phi \rightarrow \frac{v}{\sqrt{2}}\delta_{i,N} + \phi$ . Parametrically, the background field scales as  $v \sim \sqrt{T}/g^n$  for some  $n \in \mathbb{R}$ , with  $[v] = 1/2$ . From the requirement that the high-temperature expansion converges, soft-scale dimension-8 contributions must be subleading compared to dimension-6. This implies (omitting factors of  $\pi$ ):

$$c_8 v^8 \sim \frac{g^8}{T} \times \frac{T^4}{g^{8n}} \ll c_6 v^6 \sim g^6 \times \frac{T^3}{g^{6n}} \iff g^{2(1-n)} \ll 1 \iff n < 1. \quad (4.2)$$

On the other hand, from the matching (see eq. (C.13)), the quartic must satisfy  $\lambda_3/T \sim g^m$  with  $2 < m < 4$ , so if we assume that dimension-6 terms enter  $V_{\text{eff}}^{\text{LO}}$ , then

$$\lambda_3 v^4 \sim c_6 v^6 \iff g^m T \times \frac{T^2}{g^{4n}} \sim g^6 \times \frac{T^3}{g^{6n}} \iff g^{6-2n+m} \sim 1 \iff n = 3 - \frac{m}{2}. \quad (4.3)$$

No value in  $2 < m < 4$  is compatible with the condition in eq. (4.2), and therefore it is only consistent to include hard-scale generated dimension-6 terms along with soft-scale quantum corrections to the effective potential.

Assuming therefore the perturbative expansion in eq. (4.1), the broken-phase field-dependent masses,

$$\begin{aligned} m_B^2 &\equiv g_3^2 v^2, & m_{B_0}^2 &\equiv m_{\text{D}}^2 + h_3 v^2, \\ m_h^2 &\equiv \partial_v^2 V^{\text{LO}}, & m_{\text{G}}^2 &\equiv v^{-1} \partial_v V^{\text{LO}}, \end{aligned} \quad (4.4)$$

enter directly into the effective potential in the broken phase

$$\begin{aligned} V_{\text{eff}}|_{\text{LO}}^{\text{bro}} &= \frac{1}{2} \mu_3^2 v^2 + \frac{1}{4} \lambda_3 v^4 - \frac{1}{6\pi} m_B^3 - \frac{1}{12\pi} m_{B_0}^3, \\ V_{\text{eff}}|_{\text{NLO}}^{\text{bro}} &= \frac{1}{(4\pi)^2} \left[ -g_3^4 v^2 \left( 1 + \ln \frac{\bar{\Lambda}_{3\text{d}}^2}{4m_B^2} \right) - \frac{1}{2} h_3^2 v^2 \left( 1 + \ln \frac{\bar{\Lambda}_{3\text{d}}^2}{4m_{B_0}^2} \right) + 3\kappa_3 m_{B_0}^2 \right], \\ V_{\text{eff}}|_{\text{N}^2\text{LO}}^{\text{bro}} &= -\frac{1}{12\pi} \left[ m_h^3 + m_{\text{G}}^3 \right], \\ V_{\text{eff}}|_{\text{dim6}}^{\text{bro}} &= \frac{1}{8} c_6 v^6. \end{aligned} \quad (4.5)$$

The potential up to NNLO can be obtained using either `DRalgo` [63] or results from [85]. In the symmetric phase, the effective potential takes the form

$$\begin{aligned} V_{\text{eff}}|_{\text{LO}}^{\text{sym}} &= -\frac{1}{12\pi} (m_{\text{D}}^2)^{\frac{3}{2}}, & V_{\text{eff}}|_{\text{NLO}}^{\text{sym}} &= \frac{3}{(4\pi)^2} \kappa_3 m_{\text{D}}^2, \\ V_{\text{eff}}|_{\text{N}^2\text{LO}}^{\text{sym}} &= -\frac{1}{6\pi} (\mu_3^2)^{\frac{3}{2}}, & V_{\text{eff}}|_{\text{dim6}}^{\text{sym}} &= 0. \end{aligned} \quad (4.6)$$

As a practical step, we recast the potential into a dimensionless form by defining the dimensionless variables

$$x \equiv \frac{\lambda_3}{g_3^2}, \quad y \equiv \frac{\mu_3^2}{g_3^4}, \quad y_D \equiv \frac{m_D^2}{g_3^4}, \quad \tilde{h}_3 \equiv \frac{h_3}{g_3^2}, \quad \tilde{\kappa}_3 \equiv \frac{\kappa_3}{g_3^2}, \quad \varphi \equiv \frac{v}{g_3}, \quad (4.7)$$

and rescaling both the effective potential  $V_{\text{eff}} \rightarrow g_3^{-6} V_{\text{eff}}$  and the scalar field background  $v \rightarrow g_3 \varphi$ . In practice, we utilize the difference between the effective potential in the broken and symmetric phases,

$$\Delta V_{\text{eff}}|_{\text{LO}} = \frac{1}{2} y \varphi^2 + \frac{1}{4} x \varphi^4 - \frac{1}{6\pi} \frac{3}{2} \varphi^3 - \frac{1}{12\pi} \left[ (y_D + \tilde{h}_3 \varphi^2)^{\frac{3}{2}} - \varphi^3 - y_D^{\frac{3}{2}} \right], \quad (4.8)$$

$$\begin{aligned} \Delta V_{\text{eff}}|_{\text{NLO}} = & \frac{1}{(4\pi)^2} \left[ -\frac{3}{2} \varphi^2 \left( 1 + \ln \frac{\bar{\Lambda}_{3d}^2}{4m_B^2} \right) - \frac{\varphi^2}{2} \left( \tilde{h}_3^2 \left( 1 + \ln \frac{\bar{\Lambda}_{3d}^2}{4m_{B_0}^2} \right) - \left( 1 + \ln \frac{\bar{\Lambda}_{3d}^2}{4m_B^2} \right) \right) \right. \\ & \left. + 3\tilde{\kappa}_3 \tilde{h}_3 \varphi^2 \right], \end{aligned} \quad (4.9)$$

$$\Delta V_{\text{eff}}|_{\text{N}^2\text{LO}} = -\frac{1}{12\pi g_3^6} \left[ (m_h^2)^{\frac{3}{2}} + (m_G^2)^{\frac{3}{2}} - 2(\mu_3^2)^{\frac{3}{2}} \right], \quad (4.10)$$

$$\Delta V_{\text{eff}}|_{\text{dim6}} = \frac{1}{8} c_6 \varphi^6, \quad (4.11)$$

where for a thermodynamic expression  $X$ , we define  $\Delta X \equiv X^{\text{bro}} - X^{\text{sym}}$  as the difference between the broken and symmetric phases. Since close to the critical temperature, the parameter  $y$  and the dimensionless field  $\varphi$  scale as  $y \sim x^{-1}$  and  $\varphi \sim x^{-1}$ , one can reorganize the effective potential in powers of  $x$

$$\frac{V_{\text{eff}}}{g_3^6} \sim \boxed{x^{-3}}_{\text{LO}} + \boxed{x^{-2}}_{\text{NLO}} + \boxed{x^{-\frac{3}{2}}}_{\text{N}^2\text{LO}} + \boxed{c_6 x^{-6}}_{\text{dim6}} + \boxed{\mathcal{O}(x^{-1})}_{\text{N}^3\text{LO}}. \quad (4.12)$$

While the  $x^{-6}$  term appears dominant, the effects of dimension-6 operators are suppressed by the associated effective parameters  $c_6 \sim g^6/\pi^4$  rendering them parametrically smaller in the gauge coupling compared to other operators.

To assess the impact of the higher-order corrections on the PT parameters, it is practical to further recast the soft-scale effective potential in a form similar to the softer-scale potential (DR-A), as it allows for the existence of analytical expressions for the critical parameters; see [38, 63, 86]. To this end, we rewrite the bracketed terms in  $\Delta V_{\text{eff}}|_{\text{LO}}$  in eq. (4.8) and  $\Delta V_{\text{eff}}|_{\text{NLO}}$  in eq. (4.9) using

$$\begin{aligned} \left[ (y_D + \tilde{h}_3 \varphi^2)^{\frac{3}{2}} - \varphi^3 - y_D^{\frac{3}{2}} \right] & \simeq (\tilde{h}_3^{3/2} - 1) \varphi^3 + \mathcal{O}(x^{-1}), \\ \varphi^2 \ln \frac{\bar{\Lambda}_{3d}^2}{4m_{B_0}^2} & \simeq \varphi^2 \ln \frac{\bar{\Lambda}_{3d}^2}{4m_B^2} - \varphi^2 \ln \tilde{h}_3 + \mathcal{O}(x^0). \end{aligned} \quad (4.13)$$

Hence, the effective potential differences of eqs. (4.8)–(4.10) are rewritten as

$$\begin{aligned}\Delta V_{\text{eff}}|_{\text{LO}} &= \frac{1}{2}y\varphi^2 + \frac{1}{4}x\varphi^4 - \frac{1}{6\pi}\mathcal{E}_1\varphi^3, \\ \Delta V_{\text{eff}}|_{\text{NLO}} &= -\frac{\varphi^2}{(4\pi)^2} \left[ \mathcal{E}_2 + \mathcal{E}_3 \ln \frac{\bar{\Lambda}_{3d}^2}{4m_B^2} \right], \\ \Delta V_{\text{eff}}|_{\text{N}^2\text{LO}} &= -\frac{1}{12\pi} \left[ (\tilde{m}_h^2)^{\frac{3}{2}} + (\tilde{m}_G^2)^{\frac{3}{2}} - 2y^{\frac{3}{2}} \right],\end{aligned}\quad (4.14)$$

using the enhancement factors

$$\mathcal{E}_1 \equiv 1 + \frac{1}{2}\tilde{h}_3^{\frac{3}{2}}, \quad \mathcal{E}_2 \equiv 1 + \frac{1}{2}\tilde{h}_3^2(1 - \ln \tilde{h}_3) + 3\tilde{\kappa}_3\tilde{h}_3, \quad \mathcal{E}_3 \equiv 1 + \frac{1}{2}\tilde{h}_3^2, \quad (4.15)$$

and the dimensionless field-dependent and enhanced scalar masses

$$\tilde{m}_h^2 \equiv \frac{m_h^2}{g_3^4} = y + 3x\varphi^2 - \frac{\mathcal{E}_1\varphi}{\pi}, \quad \tilde{m}_G^2 \equiv \frac{m_G^2}{g_3^4} = y + x\varphi^2 - \frac{\mathcal{E}_1\varphi}{2\pi}. \quad (4.16)$$

In eq. (4.11), we isolate the contribution of the dimension-6 operators, as their effect on equilibrium quantities varies significantly with  $x$ . As mentioned above, we treat this contribution as subleading relative to the LO effective potential to maintain EFT consistency, as discussed in eqs. (4.2) and (4.3). At the same time, we remain agnostic about its precise perturbative order and retain only the linear correction in  $c_6$ . To determine the critical temperature  $T_c$  or, equivalently, the critical mass  $y_c$ , we find the values of  $y$  and  $x$  for which the free energies in the two phases coincide, *viz.*

$$\Delta F(y_c(x), x) = [F_{\text{bro}} - F_{\text{sym}}](y_c(x), x) = 0, \quad (4.17)$$

where the free energy density is defined as

$$F = V_{\text{eff}}(v_{\min}), \quad (4.18)$$

with  $v_{\min}$  denoting the global minimum of the effective potential. In the broken phase, it can be expanded as  $v_{\min} = [v_0 + v_1 + v_2 + \dots]$ , where  $v_0 = g_3\varphi_0$  is the LO minimum,

$$\varphi_0 = \frac{1 + \sqrt{1 - (4\pi)^2 xy}}{4\pi x}. \quad (4.19)$$

The entropy difference,  $\Delta S = \frac{d}{d \ln T} \Delta F(y, x)$ , characterizes the released amount of latent heat and therefore the transition strength. Defining the quadratic and quartic scalar condensates [28]

$$\Delta \langle \phi^\dagger \phi \rangle \equiv \partial_y \Delta F, \quad \Delta \langle (\phi^\dagger \phi)^2 \rangle \equiv \partial_x \Delta F, \quad (4.20)$$

and using the chain-rule, the entropy difference can be expressed as [87]

$$\Delta S = \left( \frac{dy}{d \ln T} \right) \Delta \langle \phi^\dagger \phi \rangle + \left( \frac{dx}{d \ln T} \right) \Delta \langle (\phi^\dagger \phi)^2 \rangle. \quad (4.21)$$

Our goal is to determine these thermodynamic parameters at the critical temperature. Accordingly, we compute  $y_c$ ,  $\Delta \langle \phi^\dagger \phi \rangle_c$ , and  $\Delta \langle (\phi^\dagger \phi)^2 \rangle_c$  order by order in  $x$ , while including the leading contribution from  $c_6$ . The resulting soft-enhanced, dimension-6 corrected expressions for the critical parameters up to  $N^2LO$ ,

$$y_c|_{N^2LO+dim6} = \frac{1}{2(3\pi)^2 x} \left[ \mathcal{E}_1^2 + \frac{9}{2} \mathcal{E}_3 x \ln \tilde{\Lambda}_{3d} - \mathcal{E}_1 \left( \frac{x}{2} \right)^{\frac{3}{2}} \right] - \frac{\mathcal{E}_1^4 c_6}{324\pi^4 x^4}, \quad (4.22)$$

$$\Delta \langle \phi^\dagger \phi \rangle_c|_{N^2LO+dim6} = \frac{1}{2(3\pi)^2 x^2} \left[ \mathcal{E}_1^2 - \frac{9}{2} \mathcal{E}_3 x + \frac{25}{2} \mathcal{E}_1 \left( \frac{x}{2} \right)^{\frac{3}{2}} \right] - \frac{\mathcal{E}_1^4 c_6}{81\pi^4 x^5}, \quad (4.23)$$

$$\Delta \langle (\phi^\dagger \phi)^2 \rangle_c|_{N^2LO+dim6} = \frac{1}{2^2(3\pi)^4 x^4} \left[ \mathcal{E}_1^4 - 9 \mathcal{E}_1^2 \mathcal{E}_3 x + 13 \mathcal{E}_1^3 \left( \frac{x}{2} \right)^{\frac{3}{2}} \right] - \frac{\mathcal{E}_1^6 c_6}{729\pi^6 x^7}, \quad (4.24)$$

depend on the 3d renormalization scale  $\tilde{\Lambda}_{3d}$  through

$$\tilde{\Lambda}_{3d} \equiv e^{\ln \frac{3}{2} + \frac{\mathcal{E}_2}{2\mathcal{E}_3}} \pi x \frac{\tilde{\Lambda}_{3d}}{\mathcal{E}_1 g_3^2}. \quad (4.25)$$

Additionally, setting  $\mathcal{E}_1 = \mathcal{E}_2 = \mathcal{E}_3 = 1$  recovers the results of [63, 76], including the dimension-6 operator contribution as in [53]. As noted in [63, 76], the scale dependence of  $y_c$  is governed by the  $\beta$ -function

$$\beta_y \equiv \partial_{t_3} y = \frac{4}{(4\pi)^2} \left[ \mathcal{E}_3 - 2x + 2x^2 \right], \quad (4.26)$$

with  $t_3 = \ln \tilde{\Lambda}_{3d}$ . We therefore define the renormalization-scale-invariant quantity

$$\tilde{y}_c \equiv y_c - \beta_y \ln \tilde{\Lambda}_{3d}. \quad (4.27)$$

Upon the substitution of our matching relations, the expressions above fully determine the critical behavior of the Abelian Higgs model to  $\mathcal{O}(g^6)$  in hard-scale and  $N^2LO + \text{dim6}$  in soft-scale contributions within perturbation theory.

#### 4.1. Comparing higher-dimensional operators against loop corrections

In this section, we assess the relative importance of higher-dimensional operators against higher-loop corrections in determining the equilibrium thermodynamics of the PT. This question is particularly relevant in the small- $x$  regime, which is phenomenologically interesting due to its correlation with stronger PTs [53]. Specifically, we want to determine the value of  $x$  beyond which, at fixed orders in  $g$ , the contribution from higher-dimensional terms dominates over higher-loop hard-scale corrections to super-renormalizable operators.

To this aim, in fig. 4 we plot the thermodynamic quantities  $\tilde{y}_c$ ,  $\Delta \langle \phi^\dagger \phi \rangle_c$ , and  $\Delta \langle (\phi^\dagger \phi)^2 \rangle_c$  with and without the leading  $c_6$  contribution, using both

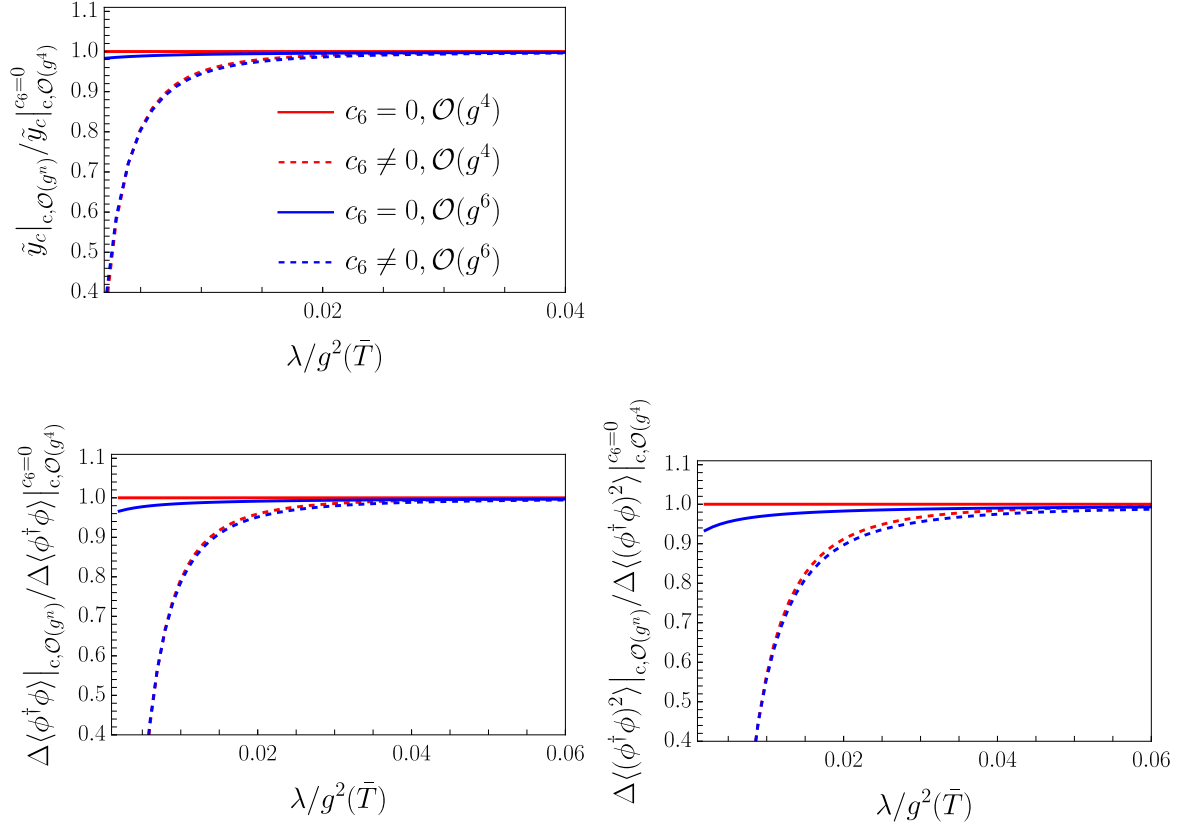


Figure 4: Relative ratios of the thermodynamic quantities  $\tilde{y}_c$ ,  $\Delta\langle\phi^\dagger\phi\rangle_c$ , and  $\Delta\langle(\phi^\dagger\phi)^2\rangle_c$  with (dashed) and without (solid) the dimension-6 contribution  $c_6$ , computed at  $\mathcal{O}(g^4)$  (red) and  $\mathcal{O}(g^6)$  (blue) matching orders. For all plots,  $T_c = 1.2$  GeV,  $g^2(\bar{T}_c) = 0.3$ ,  $\bar{\Lambda} = \bar{T}_c \equiv 4\pi e^{\gamma_E} T$ , and  $\bar{\Lambda}_{3d,\text{opt}} = 2.85 T_c$  [64].

- $\mathcal{O}(g^4)$  matching with two-loop masses and one-loop couplings,
- $\mathcal{O}(g^6)$  matching with three-loop masses and two-loop couplings.

As seen in all panels of fig. 4, for small values of  $\lambda/g^2 = x_{\text{LO}}$ , corrections induced by the  $(\phi^\dagger\phi)^3$  operator exceed those from three-loop hard-scale diagrams. This small- $x$  regime, where higher-dimensional operators dominate, also corresponds to stronger PTs, as shown in [28, 46, 53, 56]. In the opposite limit of larger  $x$ , the situation is reversed, with higher-loop corrections dominating over the effects of higher-dimensional operators. Quantitatively, this transition occurs only around  $x_{\text{LO}} \sim 1$  which is well beyond the critical endpoint of the theory which is expected to be close to the value of the critical endpoint in the softer scale EFT (DR-A) located at  $\bar{x}_c \approx 0.28$  [88, 89].<sup>4</sup>

<sup>4</sup>In contrast, the exact location of the soft-EFT critical endpoint  $x_c$  is expected to shift slightly in compar-

Furthermore, fig. 5 displays the transition strength at the critical temperature,

$$\alpha_c \approx \frac{g_3^6 \Delta S}{3p_0'} \Big|_{T_c}, \quad (4.28)$$

where the field-independent pressure  $p_0 = \frac{\pi^2}{90} g_{\text{eff}} T^4$  is also known as the unit-operator [10], with  $g_{\text{eff}}$  denoting the number of relativistic degrees of freedom in the Abelian Higgs model, namely  $g_{\text{eff}} = 4$ . We extend this analysis across a wider region of parameter space and compute the ratio of corrections from dimension-6 operators with  $c_6 \neq 0$  to those from  $\mathcal{O}(g^6)$  higher-loop matching, both relative to the  $\mathcal{O}(g^4)$  baseline without higher-dimensional operators; cf. fig. 5 (right). To this end, we define

$$\delta_{[c_6, \mathcal{O}(g^6)]} \equiv \frac{\delta \alpha_{c, \mathcal{O}(g^6)}^{c_6 \neq 0}}{\delta \alpha_{c, \mathcal{O}(g^6)}^{c_6=0}} \equiv \frac{\alpha_{c, \mathcal{O}(g^6)}^{c_6 \neq 0} - \alpha_{c, \mathcal{O}(g^4)}^{c_6=0}}{\alpha_{c, \mathcal{O}(g^6)}^{c_6=0} - \alpha_{c, \mathcal{O}(g^4)}^{c_6=0}}. \quad (4.29)$$

Fig. 5 (left) shows the baseline transition strength at the critical temperature computed using  $\mathcal{O}(g^4)$  matching while neglecting dimension-6 operators.

As shown in fig. 5 (right), corrections from higher-dimensional operators dominate over those from higher-loop matching in the parameter space associated with stronger PTs. This ratio increases as we approach regions of enhanced transition strength, indicating that the effects of higher-dimensional operators become increasingly significant in this regime, consistent with the discussion in fig. 4.

While the analysis presented here is specific for the critical temperature, we verify that by varying the temperature close to the critical temperature between  $T_c \rightarrow [10^{-2}, 10^{-1}] \times T_c$ , similar conclusions should hold at the nucleation temperature  $T_n < T_c$ . In fact, we find that  $\delta_{[c_6, \mathcal{O}(g^6)]}$  reaches up to  $\mathcal{O}(10)$ .

Finally, we comment on the implications of our findings for classically conformal gauge-Higgs models. In the conformal limit where the zero-temperature mass parameter  $\mu^2$  vanishes and the PT scale is generated dynamically by thermal effects, the Abelian Higgs model [92] with  $\lambda \ll g^2$  exhibits significantly enhanced transition strength  $\alpha_c$  in the lower left corner of fig. 5. However, nucleation occurs at the escape point of the bubble trajectory, where field values are typically much smaller than the broken-phase minimum [43]. Hence, at  $T_n$ , higher-dimensional operator effects are expected to be less pronounced and less dominant over higher loop effects in this class of models, and we defer a detailed study to future work. Nevertheless, such contributions, not included in recent studies [69, 93], remain important for accurate GW predictions and primordial black hole formation from supercooled transitions [74, 75, 94, 95].

---

ison to  $\bar{x}_c$  when including dynamical temporal scalars  $B_0$  as seen from the full 4d theory [90, 91].

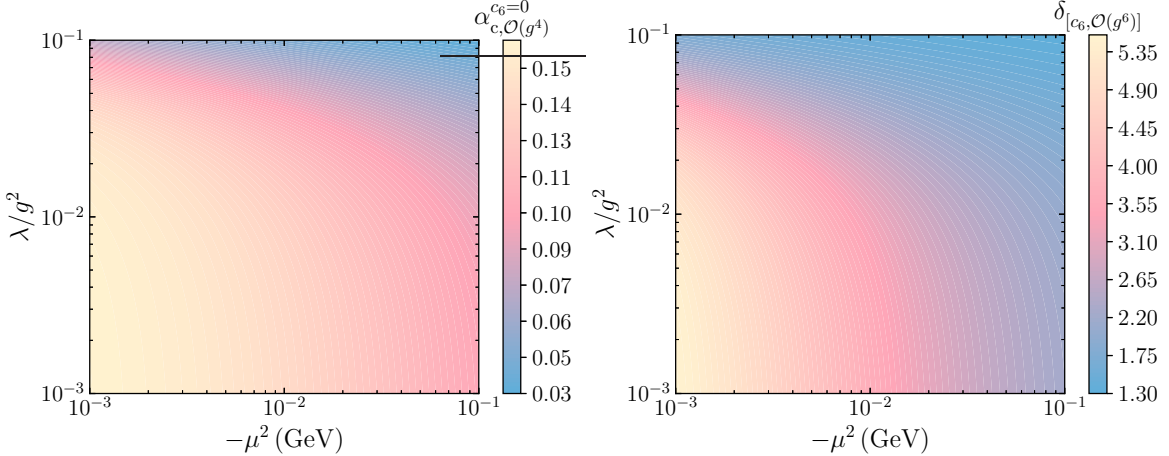


Figure 5: Left: Transition strength  $\alpha_c$  at the critical temperature (4.28), computed using  $\mathcal{O}(g^4)$  matching while neglecting dimension-6 operators. Right: Ratio of corrections from higher-dimensional operators ( $c_6 \neq 0$ ) to those from  $\mathcal{O}(g^6)$  higher-loop matching as defined in eq. (4.29). The four-dimensional couplings are fixed as in (BM1).

## 5. Outlook

In this work, we have computed hard thermal corrections to the equilibrium thermodynamics of the Abelian Higgs model at high temperatures. This computation includes the three-loop corrections to the Debye and scalar masses, as well as the four-point gauge-scalar correlators at two-loop level. These results complete the determination of the effective parameters of the dimensionally reduced EFT at  $\mathcal{O}(g^6)$  accuracy.

For the three-loop scalar mass, we identify a previously absent contribution in the master integral basis of [64, 96]. While no new sum-integrals emerge at this order and gauge-parameter invariance is preserved, renormalizability necessitates these new contributions.

Using these results, we have assessed the relative importance of higher-loop corrections against higher-dimensional operators in determining the equilibrium thermodynamics of the PT. We found that higher-dimensional operators dominate in the small- $x$  regime, with  $x_{\text{LO}} \sim \lambda/g^2$ , which is phenomenologically interesting due to the presence of stronger PTs. As expected, this dominance occurs only for values of  $x$  significantly smaller than those corresponding to the critical endpoint of the theory where loop corrections dominate instead. Our results pave the way for future studies of the nonequilibrium dynamics of the PT at  $\mathcal{O}(g^6)$  accuracy, including the computation of the bubble nucleation rate.

Our results are based on the effective potentials of [38, 63], which apply directly to the softer-scale EFT (DR-A) up to  $N^4\text{LO}$  accuracy. A natural next step beyond the soft enhancement of the softer-scale EFT used in sec. 3 is to improve the soft-scale EFT (DR-B)

by including temporal gauge-field loop contributions, following [63], again up to  $N^4\text{LO}$  accuracy. Additionally, our results motivate including higher-order EFT corrections and further investigating broad-temperature frameworks [14, 59, 97] to study PTs in BSM extensions in the strongest regimes.

## Acknowledgements

We thank Oliver Gould, Maciej Kierkla, Pablo Navarrete, Tuomas V.I. Tenkanen, York Schröder, and Jorinde van de Vis for enlightening discussions. FB and PS are supported by the Swiss National Science Foundation (SNSF) under grant PZ00P2-215997. MC is supported by the European Research Council under grant agreement n. 101230200. LG is supported by the FPU program under grant number FPU23/02026 and also acknowledges the support of the European Consortium for Astroparticle Theory in the form of an Exchange Travel Grant. This work has received further funding from MICIU/AEI/10.13039/ 501100011033 (grants PID2022-139466NB-C21/C22 and PID2024-161668NB-100) as well as from Junta de Andalucía (grants FQM 101 and P21-00199).

**Data availability statement.** The effective potential expressions used to produce figs. 3, 4, and 5 are publicly available via the software `DRalgo` [63]. Diagrams were generated with `Axodraw` [98].

## A. Renormalization group equations

For completeness, in this appendix we present the renormalization group (RG) equations of the 4d Abelian Higgs model, that we compute in the  $\overline{\text{MS}}$  scheme.

The 4d bare Lagrangian is defined as

$$\begin{aligned} \mathcal{L}^{(B)} = & \frac{1}{4} F_{\mu\nu}^{(B)} F_{\mu\nu}^{(B)} + (D_\mu \phi^{(B)})^\dagger (D_\mu \phi^{(B)}) + \mu^{2(B)} (\phi^{\dagger(B)} \phi^{(B)}) + \lambda^{(B)} (\phi^{\dagger(B)} \phi^{(B)})^2 \\ & + \frac{1}{2\xi^{(B)}} (\partial_\mu B_\mu^{(B)})^2, \end{aligned} \quad (\text{A.1})$$

with  $D_\mu^{(B)} = \partial_\mu - ig^{(B)} B_\mu^{(B)}$ . The bare fields and parameters are related to the renormalized ones by

$$\begin{aligned} \phi^{(B)} &= Z_s^{1/2} \phi, & B_\mu^{(B)} &= Z_B^{1/2} B_\mu, & \mu^{2(B)} &= \mu^2 Z_{\mu^2}, \\ \lambda^{(B)} &= \lambda \Lambda^{2\epsilon} Z_\lambda, & g^{2(B)} &= g^2 \Lambda^{2\epsilon} Z_{g^2}, & \xi^{(B)} &= \xi Z_\xi, \end{aligned} \quad (\text{A.2})$$

with  $\bar{\Lambda}$  being the  $\overline{\text{MS}}$  scheme scale defined as  $\bar{\Lambda}^2 = 4\pi e^{-\gamma_E} \Lambda^2$ , and  $\gamma_E$  being the Euler-Mascheroni constant. At two-loop order,<sup>5</sup> the normalization factors are

$$\begin{aligned}
Z_s &= 1 + \frac{1}{(4\pi)^2} \frac{1}{\epsilon} (3 - \xi) g^2 + \frac{1}{(4\pi)^4} \left[ \frac{10 - 6\xi + \xi^2}{2\epsilon^2} g^4 + \frac{1}{3\epsilon} (-5g^4 - 6\lambda^2) \right], \\
Z_B &= 1 - \frac{1}{(4\pi)^2} \frac{1}{\epsilon} \frac{1}{3} g^2 + \frac{1}{(4\pi)^4} \left[ -\frac{2}{\epsilon} g^4 \right], \\
Z_\xi &= Z_B, \\
Z_{g^2} &= 1 + \frac{1}{(4\pi)^2} \frac{1}{\epsilon} \frac{1}{3} g^2 + \frac{1}{(4\pi)^4} \left[ \frac{1}{9\epsilon^2} g^4 + \frac{2}{\epsilon} g^4 \right], \\
\lambda Z_\lambda &= \lambda + \frac{1}{(4\pi)^2} \frac{1}{\epsilon} \left( 10\lambda^2 - 6g^2\lambda + 3g^4 \right) + \frac{1}{(4\pi)^4} \left[ \frac{1}{\epsilon^2} \left( 100\lambda^3 - 90g^2\lambda^2 + 47g^4\lambda - 8g^6 \right) \right. \\
&\quad \left. + \frac{1}{\epsilon} \left( -60\lambda^3 + 28g^2\lambda^2 + \frac{79}{3}g^4\lambda - \frac{52}{3}g^6 \right) \right], \\
Z_{\mu^2} &= 1 + \frac{1}{(4\pi)^2} \frac{1}{\epsilon} \left( 4\lambda - 3g^2 \right) \\
&\quad + \frac{1}{(4\pi)^4} \left[ \frac{1}{\epsilon^2} \left( 28\lambda^2 - 24g^2\lambda + 10g^4 \right) + \frac{1}{\epsilon} \left( -10\lambda^2 + 16g^2\lambda + \frac{43}{6}g^4 \right) \right]. \tag{A.3}
\end{aligned}$$

As a crosscheck, we verify that  $Z_{g^2} = (Z_B)^{-1}$  and  $Z_\xi = Z_B$ , according to gauge invariance. The related  $\beta$ -functions are

$$\begin{aligned}
\beta_{g^2} &\equiv \partial_t g^2 = \frac{1}{(4\pi)^2} \left[ \frac{2}{3} g^4 \right] + \frac{1}{(4\pi)^4} \left[ 8g^6 \right], \\
\beta_\lambda &\equiv \partial_t \lambda = \frac{1}{(4\pi)^2} \left[ 6g^4 - 12g^2\lambda + 20\lambda^2 \right] \\
&\quad + \frac{1}{(4\pi)^4} \left[ -\frac{208}{3}g^6 + \frac{316}{3}g^4\lambda + 112g^2\lambda^2 - 240\lambda^3 \right], \\
\gamma_{\mu^2} &\equiv \frac{\partial_t \mu^2}{\mu^2} = \frac{1}{(4\pi)^2} \left[ -6g^2 + 8\lambda \right] \\
&\quad + \frac{1}{(4\pi)^4} \left[ -40\lambda^2 + 64g^4\lambda + \frac{86}{3}g^4 \right], \tag{A.4}
\end{aligned}$$

with  $t \equiv \ln \bar{\Lambda}$ .

## B. Master integrals

In the following, we use the same notation as in [99], and we present all our sum-integral results in the  $\overline{\text{MS}}$  scheme in dimensional regularization, with  $d = 3 - 2\epsilon$ . We adopt the usual

---

<sup>5</sup>The  $Z$ -factors presented here remain valid at three-loop level to  $\mathcal{O}(g^6)$ , as  $Z_{\mu^2}$  receives no additional running corrections at this order.

notation for sum-integrals

$$\oint_K \equiv T \sum_{n=-\infty}^{\infty} \int_{\mathbf{k}}, \quad \int_{\mathbf{k}} \equiv \Lambda^{3-d} \int \frac{d^d \mathbf{k}}{(2\pi)^d}, \quad (\text{B.1})$$

where  $K = (k_0, \mathbf{k}) = (k_n, \mathbf{k})$  is a loop 4-momentum, and  $n \in \mathbb{Z}$  labels the bosonic Matsubara modes with zero-momenta  $k_n = 2\pi n T$  running in the loop. We use a basis of sum-integrals of the form

$$\mathcal{I}_s^\alpha = \oint_K \frac{(k_0)^\alpha}{[K^2]^s}, \quad (\text{B.2})$$

$$\mathcal{I}_{s_1 s_2 s_3}^{\alpha_1 \alpha_2} = \oint_{K_1 K_2} \frac{(k_{1,0})^{\alpha_1} (k_{2,0})^{\alpha_2}}{[K_1^2]^{s_1} [K_2^2]^{s_2} [(K_1 - K_2)^2]^{s_3}}, \quad (\text{B.3})$$

$$\mathcal{I}_{s_1 s_2 s_3 s_4 s_5 s_6}^{\alpha_1 \alpha_2 \alpha_3} = \oint_{K_1 K_2 K_3} \frac{(k_{1,0})^{\alpha_1} (k_{2,0})^{\alpha_2} (k_{3,0})^{\alpha_3}}{[K_1^2]^{s_1} [K_2^2]^{s_2} [K_3^2]^{s_3} [(K_1 - K_2)^2]^{s_4} [(K_1 - K_3)^2]^{s_5} [(K_2 - K_3)^2]^{s_6}}. \quad (\text{B.4})$$

At one- and two-loop level, master integrals factorize into one-loop thermal integrals of the type (B.2); see [100, 101] for a proof. Full bosonic integrals without Matsubara modes in the numerator are abbreviated with  $\mathcal{I}_{s_1 \dots s_n}^{0 \dots 0} \equiv \mathcal{I}_{s_1 \dots s_n}$ .

At three-loop level, there exist master integrals which do not factorize into lower-loop cases. We use an in-house Laporta algorithm [102] adapted to finite temperature [103, 104] to reduce integrals to a finite set of master integrals [105] via integration by parts (IBP). Once a basis of master integrals is found, further exploitation of IBP relations can also allow us to change the basis of master integrals to evaluate. This becomes a necessity in the evaluation of the three-loop thermal masses, as discussed in sec. C.1 and [56]. After these manipulations, the remaining sum-integrals in eq. (C.36) can be addressed using classic [81, 106–108] and modern methods [59, 109, 110]. While the procedure is, in principle, straightforward, it is technically demanding. An explicit algorithm for evaluating the basketball-type integrals was developed in [111], illustrated with the example of  $\mathcal{I}_{310011}^{200}$ . For the present calculation, the dimension-two three-loop basketball master integral  $\mathcal{I}_{110011}$  is known from [107],  $\mathcal{I}_{210011}$  from [112, 113], and the corresponding spectacles-type integrals were tamed in [64, 81, 108]. The different spectacle-type integrals were evaluated in [114, 115] for  $\mathcal{I}_{111110}$ , [96] for  $\mathcal{I}_{211110}^{020}$ , and [81] for  $\mathcal{I}_{31111-2}$ . Here, we collect the evaluated expressions for these integrals that also form the master integral basis (C.36),

$$\begin{aligned} \mathcal{I}_{210011} = \frac{T^2}{(4\pi)^4} \left( \frac{1}{4\pi T^2} \right)^{3\epsilon} \frac{1}{8\epsilon^2} & \left[ 1 + \left( \frac{17}{6} + \gamma_E + 2Z'_1 \right) \epsilon \right. \\ & \left. + \left( \frac{131}{12} + \frac{31\pi^2}{36} + 8\ln(2\pi) - \frac{9\gamma_E}{2} - \frac{15\gamma_E^2}{2} + (5 + 2\gamma_E)Z'_1 \right) \right] \end{aligned} \quad (\text{B.5})$$

$$+ 2Z_1'' - 16\gamma_1 + \frac{4\zeta_3}{9} - 0.145652981107(4)\Big) \epsilon^2 + \mathcal{O}(\epsilon^3)\Big],$$

$$\begin{aligned} \mathcal{I}_{111110} = & -\frac{T^2}{(4\pi)^4} \left(\frac{1}{4\pi T^2}\right)^{3\epsilon} \frac{1}{4\epsilon^2} \left[ 1 + \left(\frac{4}{3} + \gamma_E + 2Z_1'\right)\epsilon \right. \\ & + \left(\frac{1}{3}\left[46 + \frac{45\pi^2}{4} + 24\ln(2\pi)(\ln(2\pi) - \gamma_E) - 104\gamma_1 - 8\gamma_E\left(\frac{5}{16}\gamma_E + 1\right) \right. \right. \\ & \left. \left. + 8(2\gamma_E + 3)Z_1' + 2Z_1''\right] - 38.53084275773721000(10)\right) \epsilon^2 + \mathcal{O}(\epsilon^3)\Big], \end{aligned} \quad (\text{B.6})$$

$$\mathcal{I}_{211110}^{020} = \frac{T^2}{(4\pi)^4} \left(\frac{1}{4\pi T^2}\right)^{3\epsilon} \frac{1}{96\epsilon^2} \left[ 1 + \left(\frac{67}{6} + \gamma_E + 2Z_1'\right)\epsilon + 93.0894417(2)\epsilon^2 + \mathcal{O}(\epsilon^3)\right], \quad (\text{B.7})$$

$$\begin{aligned} \mathcal{I}_{31111-2} = & -\frac{T^2}{(4\pi)^4} \left(\frac{1}{4\pi T^2}\right)^{3\epsilon} \frac{5}{36\epsilon^2} \left[ 1 + \left(\frac{71}{30} + \gamma_E + 2Z_1'\right)\epsilon + 44.629857(1)\epsilon^2 + \mathcal{O}(\epsilon^3)\right] \\ & + \delta\mathcal{I}_{31111-2}. \end{aligned} \quad (\text{B.8})$$

Here,  $\gamma_1$  is the first of the Stieltjes constants defined via  $\zeta_s = (s-1)^{-1} + \sum_{n=0}^{\infty} (1-s)^n \gamma_n / n!$ , and  $\zeta_s \equiv \zeta(s)$  is the Riemann  $\zeta$ -function. We also abbreviate derivatives of the  $\zeta$ -function by  $Z_s^{(n)} = \zeta_{-s}^{(n)} / \zeta_{-s}$ . Finally, we introduced the modification  $\delta\mathcal{I}_{31111-2}$  in eq. (3.10) to ensure renormalizability of the three-loop scalar mass result in eq. (3.6).

### C. Details of dimensional reduction

In this section, we collect all matching relations and expressions of the effective parameters in the soft-scale EFT (DR-B). The 3d EFT bare<sup>6</sup> Lagrangian is given by

$$\begin{aligned} \mathcal{L}_{\text{soft}}^{(B)} = & \frac{1}{4} F_{ij}^{(B)} F_{ij}^{(B)} + (D_i \phi^{(B)})^\dagger (D_i \phi^{(B)}) + \hat{\mu}_3^{2(B)} (\phi^{\dagger(B)} \phi^{(B)}) + \frac{1}{2} (\partial_i B_0^{(B)})^2 + \frac{1}{2} \hat{m}_{\text{D}}^{2(B)} (B_0^{(B)})^2 \\ & + \hat{\lambda}_3^{(B)} (\phi^{\dagger(B)} \phi^{(B)})^2 + \hat{h}_3^{(B)} (\phi^{\dagger(B)} \phi^{(B)}) (B_0^{(B)})^2 + \hat{\kappa}_3^{(B)} (B_0^{(B)})^4 + \frac{1}{2\xi} (\partial_\mu B_\mu^{(B)})^2 + \mathcal{L}_{\text{soft}}^{(6)}, \end{aligned} \quad (\text{C.1})$$

where  $D_i = \partial_i - i \hat{g}_3 B_i^{(B)}$ . The  $\mathcal{L}_{\text{soft}}^{(6)}$  piece contains an off-shell basis of dimension-6 operators, listed in tab. 1. Hatted effective parameters indicate this off-shell basis; they shift under the field redefinitions to the on-shell physical basis discussed below.

---

<sup>6</sup>Here, by *bare* we mean that the matching equations do not include the corresponding counterterms in the 3d EFT. 4d renormalization of these results is omitted for brevity. To get a finite result, we replace each bare 4d parameter  $c_i^{(B)} \rightarrow c_i - \delta c_i$  by its renormalized counterpart perturbatively.

dimension-6 operator basis		Redundant operators	
$F_{ij}F_{ij}B_0^2$	$\hat{\alpha}_{B_0^2 F^2}$	$(\partial_i F_{ij})^2$	$\hat{\alpha}_{D^2 F^2}$
$F_{ij}F_{ij}\phi^\dagger\phi$	$\hat{\alpha}_{\phi^2 F^2}$	$B_0 \square^2 B_0$	$\hat{\alpha}_{D^4 B_0^2}$
$(D_i\phi^\dagger D_i\phi)(\phi^\dagger\phi)$	$\hat{\alpha}_{D^2\phi^4,1}$	$B_0^3 \square B_0$	$\hat{\alpha}_{D^2 B_0^4}$
$(D_i\phi^\dagger D_i\phi)B_0^2$	$\hat{\alpha}_{D^2\phi^2 B_0^2,3}$	$(D^2\phi^\dagger)(D^2\phi)$	$\hat{\alpha}_{D^4\phi^2}$
$B_0^6$	$\hat{\alpha}_{B_0^6}$	$(\phi^\dagger\phi)(\phi^\dagger D^2\phi + h.c.)$	$\hat{\alpha}_{D^2\phi^4,2}$
$B_0^4(\phi^\dagger\phi)$	$\hat{\alpha}_{\phi^2 B_0^4}$	$(\partial_i F_{ij})i\phi^\dagger(D_j\phi)$	$\hat{\alpha}_{D^2\phi^2 F}$
$B_0^2(\phi^\dagger\phi)^2$	$\hat{\alpha}_{\phi^4 B_0^2}$	$(\phi^\dagger\phi)B_0 \square B_0$	$\hat{\alpha}_{D^2\phi^2 B_0^2,1}$
$(\phi^\dagger\phi)^3$	$\hat{\alpha}_{\phi^6}$	$\phi^\dagger(D_i^2\phi)B_0^2 + h.c.$	$\hat{\alpha}_{D^2\phi^2 B_0^2,2}$

Table 1: Off-shell basis of dimension-6 operators in the soft-scale 3d effective theory in terms of bare fields and couplings; cf. also [53].

The matching relations for the bare Wilson coefficients up to  $\mathcal{O}(g^6)$ ,

$$\begin{aligned}
Z_{\phi_3} = Z_\phi & \left\{ 1 + (\xi - 3) g^2 \mathcal{I}_2 + \frac{24(d-4)(d-3)}{(d-7)(d-5)(d-2)d} \lambda^2 (\mathcal{I}_2)^2 + \left( \frac{10}{3} - 2\xi \right) g^2 \mu^2 \mathcal{I}_3 \right. \\
& + \left( \frac{40}{3} - 8\xi \right) g^2 \lambda \mathcal{I}_1 \mathcal{I}_3 + g^4 \left[ \left( \frac{2(72 - 84d - 23d^2 + 5d^3)}{3(d-7)d} - 2d\xi \right) \mathcal{I}_1 \mathcal{I}_3 \right. \\
& \left. \left. + \left( \frac{192 - 752d + 583d^2 - 142d^3 + 11d^4}{2(d-7)(d-5)(d-2)d} - 3\xi + \frac{1}{2}\xi^2 \right) (\mathcal{I}_2)^2 \right] \right\}, \tag{C.2}
\end{aligned}$$

$$\begin{aligned}
Z_{B_0} = Z_B & \left\{ 1 + \frac{1}{3}(4-d)g^2 \mathcal{I}_2 + \frac{2}{3}(d-6)g^2 \mu^2 \mathcal{I}_3 \right. \\
& \left. - \frac{4(d-4)(d-3)(d^2 - 4d - 3)}{(d-7)(d-5)(d-2)d} g^4 (\mathcal{I}_2)^2 + \frac{2}{3}(d-6)g^2 \left[ dg^2 + 4\lambda \right] \mathcal{I}_1 \mathcal{I}_3 \right\}, \tag{C.3}
\end{aligned}$$

$$\begin{aligned}
Z_{B_i} = Z_B & \left\{ 1 + \frac{1}{3}g^2 \mathcal{I}_2 - \frac{2}{3}g^2 \mu^2 \mathcal{I}_3 \right. \\
& \left. + \frac{24(d-4)(d-3)}{(d-7)(d-5)(d-2)d} g^4 (\mathcal{I}_2)^2 - \frac{2}{3}g^2 \left[ dg^2 + 4\lambda \right] \mathcal{I}_1 \mathcal{I}_3 \right\}, \tag{C.4}
\end{aligned}$$

$$\begin{aligned}
\hat{\mu}_3^2 = \mu^2 & + \left[ dg^2 + 4\lambda \right] \mathcal{I}_1 + \left[ 3g^2 - 4\lambda \right] \mu^2 \mathcal{I}_2 + \left[ 4\lambda + \left( -\frac{10}{3} + \xi \right) g^2 \right] \mu^4 \mathcal{I}_3 \\
& + \left[ (2+d)g^4 - 4(d-3)g^2\lambda - 16\lambda^2 \right] \mathcal{I}_1 \mathcal{I}_2 \\
& + \left[ 32\lambda^2 + \left( \frac{8}{3}(3d-10) + 8\xi \right) g^2\lambda - \left( \frac{4(36 - 42d - 29d^2 + 5d^3)}{3(d-7)d} - 2d\xi \right) g^4 \right] \mu^2 \mathcal{I}_1 \mathcal{I}_3 \\
& + \left[ \frac{-96 - 254d + 89d^2 + 68d^3 - 25d^4 + 2d^5}{(d-7)(d-5)(d-2)d} g^4 \right. \\
& \left. - \frac{8(d-6)(d-1)}{(d-5)(d-2)} g^2\lambda + \frac{16(d^2 - 7d - 2)(d^2 - 7d + 9)}{(d-7)(d-5)(d-2)d} \lambda^2 \right] \mu^2 (\mathcal{I}_2)^2
\end{aligned}$$

$$\begin{aligned}
& - \left[ \frac{96(d-4)(d-3)}{(d-7)(d-5)(d-2)d} \lambda^3 + \left( \frac{24(2d^3 - 27d^2 + 111d - 128)}{(d-7)(d-5)(d-2)} - 16\xi \right) g^2 \lambda^2 \right. \\
& + \left( \frac{2(192 + 508d - 899d^2 + 464d^3 - 91d^4 + 6d^5)}{(d-7)(d-5)(d-2)d} - 4d\xi + 2\xi^2 \right) g^4 \lambda \\
& + \left. \left( \frac{(d-3)(5d^3 - 55d^2 + 232d - 344)}{2(d-2)(d-5)(d-7)} - 2(d-1)\xi + \frac{1}{2}d\xi^2 \right) g^6 \right] \mathcal{I}_1(\mathcal{I}_2)^2 \\
& - \left[ \left( \frac{160}{3} - 32\xi \right) g^2 \lambda^2 + \left( \frac{16(36 - 42d - 29d^2 + 5d^3)}{3d(d-7)} - 16d\xi \right) g^4 \lambda \right. \\
& + \left. \left( \frac{2(72 - 84d - 23d^2 + 5d^3)}{3(d-7)} - 2d^2\xi \right) g^6 \right] (\mathcal{I}_1)^2 \mathcal{I}_3 + \Pi_{\phi^\dagger \phi}^{3\ell,(B)}, \tag{C.5}
\end{aligned}$$

$$\begin{aligned}
\hat{m}_D^2 = & 2(d-1)g^2 \mathcal{I}_1 - 2(d-3)g^2 \mu^2 \mathcal{I}_2 - \left[ \frac{4}{3}(d^2 - 2d - 2)g^4 + 8(d-3)g^2 \lambda \right] \mathcal{I}_1 \mathcal{I}_2 \\
& - \left[ \frac{2(d-3)(d^2 - 9d + 26)}{3(d-2)} g^4 - 8(d-3)g^2 \lambda \right] \mu^2 (\mathcal{I}_2)^2 + 2(d-5)g^2 \mu^4 \mathcal{I}_3 \\
& - \frac{4}{3}(d-6)(d-1) \left[ dg^6 + 4\lambda g^4 \right] (\mathcal{I}_1)^2 \mathcal{I}_3 - \frac{4}{3}(d-4) \left[ 2(d-3)g^4 \lambda \right. \\
& + \left. \frac{162d + 140d - 266d^2 - 16d^3 + 67d^4 - 16d^5 + d^6}{3(d-7)(d-5)(d-2)d} g^6 \right] \mathcal{I}_1 (\mathcal{I}_2)^2 \\
& + \left[ \frac{8}{3}(d^2 - 4d - 3)g^4 + 16(d-5)g^2 \lambda \right] \mu^2 \mathcal{I}_1 \mathcal{I}_3 + \Pi_{B_0 B_0}^{3\ell,(B)}, \tag{C.6}
\end{aligned}$$

$$\begin{aligned}
\frac{\hat{\lambda}_3}{T} = & \lambda + \left[ -dg^4 - 10\lambda^2 + 6g^2 \lambda \right] \mathcal{I}_2 + \left[ -\frac{2(3d^3 - 20d^2 + 27d + 10)}{(d-5)(d-2)} g^6 \right. \\
& - \frac{2(282 - 217d + 31d^2)}{(d-5)(d-2)} g^2 \lambda^2 + \frac{4(9d^4 - 126d^3 + 487d^2 - 322d - 144)}{(d-7)(d-5)(d-2)d} \lambda^3 \\
& + \left. \frac{8d^5 - 95d^4 + 210d^3 + 619d^2 - 1390d - 192}{(d-7)(d-5)(d-2)d} g^4 \lambda \right] (\mathcal{I}_2)^2 + 20 \left[ \lambda^2 - \frac{1}{3}g^2 \lambda \right] \mu^2 \mathcal{I}_3 \\
& + \left[ 4(d-1)g^6 + 80\lambda^3 + \frac{20}{3}(3d-4)g^2 \lambda^2 - \frac{4(72 - 84d - 23d^2 + 5d^3)}{3(d-7)d} g^4 \lambda \right] \mathcal{I}_1 \mathcal{I}_3, \tag{C.7}
\end{aligned}$$

$$\begin{aligned}
\frac{\hat{h}_3}{T} = & g^2 - \left[ \frac{1}{3}(2d-5)g^4 + 4(d-3)g^2 \lambda \right] \mathcal{I}_2 + \left( \frac{2}{3}g^4 \mu^2 + 8(d-5)g^2 \lambda \mu^2 \right) \mathcal{I}_3 \\
& + \left[ \frac{-2160 - 9274d + 12805d^2 - 7372d^3 + 2191d^4 - 310d^5 + 16d^6}{9(d-7)(d-5)(d-2)d} g^6 \right. \\
& - \frac{4(d-4)(d-3)(28-d+d^2)}{3(d-5)(d-2)} g^4 \lambda \\
& + \left. \frac{16(-3+d)(6-27d+45d^2-13d^3+d^4)}{d(d-7)(d-5)(d-2)} g^2 \lambda^2 \right] (\mathcal{I}_2)^2 \\
& + \left[ \frac{2(-72 + 96d - 31d^2 + d^3)}{3(d-7)d} g^6 + \frac{8}{3}(3d^2 - 15d + 1)g^4 \lambda + 32(d-5)g^2 \lambda^2 \right] \mathcal{I}_1 \mathcal{I}_3, \tag{C.8}
\end{aligned}$$

$$\begin{aligned} \frac{\widehat{g}_3^2}{T} &= g^2 - \frac{1}{3}g^4 \mathcal{I}_2 + \frac{d^4 - 14d^3 - 157d^2 + 1442d - 2592}{9(d-7)(d-5)(d-2)d} g^6 (\mathcal{I}_2)^2 \\ &\quad + \frac{2}{3}g^4 \mu^2 \mathcal{I}_3 + \frac{2}{3} \left[ dg^6 + 4g^4 \lambda \right] \mathcal{I}_1 \mathcal{I}_3, \end{aligned} \quad (\text{C.9})$$

$$\begin{aligned} \frac{\widehat{\kappa}_3}{T} &= -\frac{1}{6}(d-3)(d-1)g^4 \mathcal{I}_2 - \left[ \frac{1}{18}(d-7)(d-3)(2d-5)g^6 - 2(d-3)^2 g^4 \lambda \right] (\mathcal{I}_2)^2 \\ &\quad - \frac{1}{3}(d-5)(d-3)g^4 \mu^2 \mathcal{I}_3 - \frac{1}{3}(d-5)(d-3)g^4 \left[ dg^2 + 4\lambda \right] \mathcal{I}_1 \mathcal{I}_3, \end{aligned} \quad (\text{C.10})$$

are given in terms of unevaluated master sum-integrals, and are explicitly gauge parameter ( $\xi$ ) dependent. We omitted the superscript  $(B)$  on the left-hand side and collected bare three-loop contributions to the scalar and Debye masses into  $\Pi_{\phi^\dagger \phi}^{3\ell, (B)}$  and  $\Pi_{B_0 B_0}^{3\ell, (B)}$ , which are discussed separately in eqs. (C.35) and (C.34).

The dimension-6 effective parameters and the field redefinitions required to change from the off-shell basis to the on-shell one are given in [53]. After these redefinitions, and truncating at  $\mathcal{O}(g^6)$ , we find the following expressions for the bare, on-shell parameters

$$\begin{aligned} \mu_3^2 &= \mu^2 + \left[ dg^2 + 4\lambda \right] \mathcal{I}_1 + \left[ (2+d)g^4 - 4(d-3)g^2 \lambda - 16\lambda^2 \right] \mathcal{I}_1 \mathcal{I}_2 \\ &\quad + \left[ 3g^2 - 4\lambda \right] \mu^2 \mathcal{I}_2 + \left[ \frac{-96 - 254d + 89d^2 + 68d^3 - 25d^4 + 2d^5}{(d-7)(d-5)(d-2)d} g^4 \right. \\ &\quad \left. - \frac{8(d-6)(d-1)}{(d-5)(d-2)} g^2 \lambda + \frac{16(d^2 - 7d - 2)(d^2 - 7d + 9)}{(d-7)(d-5)(d-2)d} \lambda^2 \right] \mu^2 (\mathcal{I}_2)^2 \\ &\quad - \left[ \frac{96(d-4)(d-3)}{(d-7)(d-5)(d-2)d} \lambda^3 + \frac{24(2d^3 - 27d^2 + 111d - 128)}{(d-7)(d-5)(d-2)} g^2 \lambda^2 \right. \\ &\quad \left. + \frac{2(192 + 508d - 899d^2 + 464d^3 - 91d^4 + 6d^5)}{(d-7)(d-5)(d-2)d} g^4 \lambda \right. \\ &\quad \left. + \frac{(d-3)(5d^3 - 55d^2 + 232d - 344)}{2(d-2)(d-5)(d-7)} g^6 \right] \mathcal{I}_1 (\mathcal{I}_2)^2 + \left[ 4\lambda - \frac{5}{3}g^2 \right] \mu^4 \mathcal{I}_3 \\ &\quad + \left[ 32\lambda^2 + \frac{8}{3}(3d-5)g^2 \lambda - \frac{2(5d^3 - 23d^2 - 84d + 72)}{3(d-7)d} g^4 \right] \mu^2 \mathcal{I}_1 \mathcal{I}_3 \\ &\quad - \left[ \frac{80}{3}g^2 \lambda^2 + \frac{8(72 - 84d - 23d^2 + 5d^3)}{3d(d-7)} g^4 \lambda + \frac{5d^3 - 11d^2 - 168 + 144}{3(d-7)} g^6 \right] (\mathcal{I}_1)^2 \mathcal{I}_3 \\ &\quad - \frac{1}{2}(dg^2 + 4\lambda) g^4 \mathcal{I}_1 (\mathcal{I}_2)^2 \xi^2 + \left\{ 2 \left[ (d-1)g^4 + 2d g^2 \lambda + 8\lambda^2 \right] g^2 \mathcal{I}_1 (\mathcal{I}_2)^2 \right. \\ &\quad \left. + \left( dg^2 + 4\lambda \right)^2 g^2 (\mathcal{I}_1)^2 \mathcal{I}_3 \right\} \xi + \Pi_{\phi^\dagger \phi}^{3\ell, (B)}, \end{aligned} \quad (\text{C.11})$$

$$\begin{aligned} m_D^2 &= 2(d-1)g^2 \mathcal{I}_1 - 2(d-3)g^2 \mu^2 \mathcal{I}_2 - \left[ \frac{4}{3}(d^2 - 2d - 2)g^4 + 8(d-3)g^2 \lambda \right] \mathcal{I}_1 \mathcal{I}_2 \\ &\quad - \left[ \frac{2(d-3)(d^2 - 9d + 26)}{3(d-2)} g^4 - 8(d-3)g^2 \lambda \right] \mu^2 (\mathcal{I}_2)^2 + 2(d-5)g^2 \mu^4 \mathcal{I}_3 \\ &\quad - \frac{4}{3}(d-6)(d-1) \left[ \frac{1}{5}(4d-1)g^6 + 4g^4 \lambda \right] (\mathcal{I}_1)^2 \mathcal{I}_3 - \frac{4}{3}(d-4) \left[ 2(d-3)g^4 \lambda \right. \\ &\quad \left. + \left( dg^2 + 4\lambda \right)^2 g^2 (\mathcal{I}_1)^2 \mathcal{I}_3 \right] \xi + \Pi_{B_0 B_0}^{3\ell, (B)}, \end{aligned}$$

$$\begin{aligned}
& + \frac{(162d + 140d - 266d^2 - 16d^3 + 67d^4 - 16d^5 + d^6)}{3(d-7)(d-5)(d-2)d} g^6 \Big] \mathcal{I}_1(\mathcal{I}_2)^2 \\
& + \left[ \frac{8}{3}(d^2 - 4d - 3)g^4 + 16(d-5)g^2\lambda \right] \mu^2 \mathcal{I}_1 \mathcal{I}_3 + \Pi_{B_0 B_0}^{3\ell, (B)}, \tag{C.12}
\end{aligned}$$

$$\begin{aligned}
\frac{\lambda_3}{T} = & \lambda + \left[ -dg^4 - 10\lambda^2 + 6g^2\lambda \right] \mathcal{I}_2 + \left[ -\frac{2(3d^3 - 20d^2 + 27d + 10)}{(d-5)(d-2)} g^6 \right. \\
& - \frac{2(282 - 217d + 31d^2)}{(d-5)(d-2)} g^2\lambda^2 + \frac{4(9d^4 - 126d^3 + 487d^2 - 322d - 144)}{(d-7)(d-5)(d-2)d} \lambda^3 \\
& + \frac{8d^5 - 95d^4 + 210d^3 + 619d^2 - 1390d - 192}{(d-7)(d-5)(d-2)d} g^4\lambda \Big] (\mathcal{I}_2)^2 + \left[ -\frac{2}{15}(13 + 5d)g^4 \right. \\
& \left. + \frac{44}{3}\lambda^2 - \frac{20}{3}g^2\lambda \right] \mu^2 \mathcal{I}_3 + \left[ -\frac{2}{15}(30 - 17d + 5d^2)g^6 + \frac{176}{3}\lambda^3 + \frac{4}{3}(11d - 20)g^2\lambda^2 \right. \\
& \left. - \frac{4(360 - 602d - 159d^2 + 35d^3)}{15(d-7)d} g^4\lambda \right] \mathcal{I}_1 \mathcal{I}_3, \tag{C.13}
\end{aligned}$$

$$\begin{aligned}
\frac{h_3}{T} = & g^2 - \left[ \frac{1}{3}(2d-5)g^4 + 4(d-3)g^2\lambda \right] \mathcal{I}_2 + \left[ -\frac{2}{3}(2d-11)g^4\mu^2 + 8(d-5)g^2\lambda\mu^2 \right] \mathcal{I}_3 \\
& + (d-3) \left[ \frac{-2160 - 9274d + 12805d^2 - 7372d^3 + 2191d^4 - 310d^5 + 16d^6}{9(d-7)(d-5)(d-3)(d-2)d} g^6 \right. \\
& - \frac{4(-4+d)(28-d+d^2)}{3(d-5)(d-2)} g^4\lambda + \frac{16(6-27d+45d^2-13d^3+d^4)}{d(d-7)(d-5)(d-2)} g^2\lambda^2 \Big] (\mathcal{I}_2)^2 \\
& + \left[ \frac{2(-360+514d+855d^2-273d^3+22d^4)}{15(d-7)d} g^6 + \frac{8}{3}(d^2-5d+1)g^4\lambda \right. \\
& \left. + 32(d-5)g^2\lambda^2 \right] \mathcal{I}_1 \mathcal{I}_3, \tag{C.14}
\end{aligned}$$

$$\begin{aligned}
\frac{g_3^2}{T} = & g^2 - \frac{1}{3}g^4 \mathcal{I}_2 + \frac{d^4 - 14d^3 - 157d^2 + 1442d - 2592}{9(d-7)(d-5)(d-2)d} g^6 (\mathcal{I}_2)^2 + \frac{2}{3}g^4\mu^2 \mathcal{I}_3 \\
& + \frac{2}{3} \left[ d g^6 + 4g^4\lambda \right] \mathcal{I}_1 \mathcal{I}_3 \Big\}, \tag{C.15}
\end{aligned}$$

$$\begin{aligned}
\frac{\kappa_3}{T} = & -\frac{1}{6}(d-3)(d-1)g^4 \mathcal{I}_2 - \left[ \frac{1}{18}(d-7)(d-3)(2d-5)g^6 - 2(d-3)^2g^4\lambda \right] (\mathcal{I}_2)^2 \\
& + \frac{1}{3}(d-5)(d-3)g^4\mu^2 \mathcal{I}_3 + (d-5) \left[ \frac{1}{9}(d^2+d-8)g^6 + \frac{4}{3}(d-3)g^4\lambda \right] \mathcal{I}_1 \mathcal{I}_3, \tag{C.16}
\end{aligned}$$

while the physical dimension-6 effective parameters are

$$\alpha_{B_0^6} = \frac{1}{45}(d-5)(d-3)(d-1)g^6 \mathcal{I}_3 T^2, \tag{C.17}$$

$$\alpha_{\phi^2 B_0^4} = \frac{1}{9} \left[ (d-5)(d-1)g^6 + 12(d-5)(d-3)g^4\lambda \right] \mathcal{I}_3 T^2, \tag{C.18}$$

$$\alpha_{\phi^4 B_0^2} = \frac{2}{15} \left[ (36d-139)g^6 + 10(35-3d)g^4\lambda + 10(13d-67)g^2\lambda^2 \right] \mathcal{I}_3 T^2, \tag{C.19}$$

$$\alpha_{\phi^6} = \frac{4}{15} \left[ 5dg^6 - (5d+3)g^4\lambda + 75g^2\lambda^2 + 100\lambda^3 \right] \mathcal{I}_3 T^2, \tag{C.20}$$

$$\alpha_{D^2\phi^2B_0^2} = \frac{1}{3}(d-4)\left[7g^4 - 4g^2\lambda\right]\mathcal{I}_3 T, \quad (\text{C.21})$$

$$\alpha_{B_0^2F^2} = -\frac{1}{6}(d-5)g^4\mathcal{I}_3 T, \quad (\text{C.22})$$

$$\alpha_{\phi^2F^2} = \frac{1}{6}\left[7g^4 - 4g^2\lambda\right]\mathcal{I}_3 T, \quad (\text{C.23})$$

$$\alpha_{D^2\phi^4} = \frac{2}{15}\left[(66-5d)g^4 + 200g^2\lambda - 20\lambda^2\right]\mathcal{I}_3 T. \quad (\text{C.24})$$

These results are consistent with (A.24)–(A.29) in [85]. The remaining residual gauge dependence in the scalar mass, cancels with the gauge-dependent contribution coming from the three-loop matching contributions.

The bare fields and parameters of the super-renormalizable part of the 3d Lagrangian are related to the renormalized ones by

$$\begin{aligned} \phi_3^{(B)} &= Z_{\phi_3}^{1/2} \phi_3, & B_i^{(B)} &= Z_{B_i}^{1/2} B_i, & B_0^{(B)} &= Z_{B_0}^{1/2} B_0, \\ \mu_3^{2(B)} &= \mu_3^2 + \delta\mu_3^2, & m_{\text{D}}^{2(B)} &= m_{\text{D}}^2 + \delta m_{\text{D}}^2, & g_3^{2(B)} &= Z_{g_3^2}(\Lambda_{3d})^{2\epsilon} g_3^2, \\ \lambda_3^{(B)} &= Z_{\lambda_3}(\Lambda_{3d})^{2\epsilon} \lambda_3, & h_3^{(B)} &= Z_{h_3}(\Lambda_{3d})^{2\epsilon} h_3, & \kappa_3^{(B)} &= Z_{\kappa_3}(\Lambda_{3d})^{2\epsilon} \kappa_3. \end{aligned} \quad (\text{C.25})$$

At super-renormalizable level, the expression for the counterterms is exact at the two-loop level. We verify that the contribution to the counterterms from higher-dimensional operators starts only at  $\mathcal{O}(g^8)$  [61]. The expressions for the 3d counterterms are [85, 116, 117]

$$Z_{g_3^2} = Z_{\lambda_3} = Z_{h_3} = Z_{\kappa_3} = 1, \quad (\text{C.26})$$

$$\delta\mu_3^2 = \frac{1}{(4\pi)^2}\frac{1}{\epsilon}\left[g_3^4 + \frac{1}{2}h_3^2 - 2g_3^2\lambda_3 + 2\lambda_3^2\right], \quad (\text{C.27})$$

$$\delta m_{\text{D}}^2 = -\frac{1}{(4\pi)^2}\frac{1}{\epsilon}\left[g_3^2h_3 - h_3^2 - 24\kappa_3^2\right]. \quad (\text{C.28})$$

Following the procedure in [64], we substitute the matching relations eqs. (C.17)–(C.24) into the expressions for the 3d couplings:

$$\begin{aligned} \delta\mu_3^2 &= \frac{T^2}{(4\pi)^2}\frac{1}{\epsilon}\left[\frac{3}{2}g^2 - 4g^2\lambda + 4\lambda^2\right]\left(\frac{\Lambda}{\bar{\Lambda}_{3d}}\right)^{4\epsilon} \\ &+ \frac{T^2}{(4\pi)^2}\frac{1}{\epsilon}\left[\left(1 + \frac{4}{3}d\right)g^6 + \left(\frac{2}{3} - 8d\right)g^4\lambda + 44g^2\lambda^2 - 40\lambda^3\right]\left(\frac{\Lambda}{\bar{\Lambda}_{3d}}\right)^{4\epsilon}\Lambda^{2\epsilon}\mathcal{I}_2 \\ &- \frac{T^2}{(4\pi)^4}\frac{1}{\epsilon^2}\left[5g^6 - \frac{70}{3}g^4\lambda + 44g^2\lambda^2 - 40\lambda^3\right]\left(\frac{\Lambda}{\bar{\Lambda}_{3d}}\right)^{4\epsilon} + \mathcal{O}(g^8), \end{aligned} \quad (\text{C.29})$$

$$\delta m_{\text{D}}^2 = -\frac{T^2}{(4\pi)^2}\frac{1}{\epsilon}(d-3)g^2(g^2+6\lambda)\left(\frac{\Lambda}{\bar{\Lambda}_{3d}}\right)^{4\epsilon}\Lambda^{2\epsilon}\mathcal{I}_2 + \mathcal{O}(g^8). \quad (\text{C.30})$$

Upon expanding about  $d = 3 - 2\epsilon$ , the double pole  $1/\epsilon^2$  of  $\delta\mu_3^2$  in eq. (C.29) cancels. The single pole removes the remaining divergence in  $\mu_3^2$  after 4d renormalization, rendering the effective scalar mass finite.

As one of the main results of this work, we now present the computation of the three-loop contributions to the scalar and Debye masses. The final renormalized expressions are given in eqs. (3.6) and (3.7).

### C.1. Three-loop thermal masses in the Abelian Higgs model

The three-loop two-point correlators for the temporal and Lorentz scalars contribute to the corresponding Debye mass (3.4) and scalar thermal mass (3.5). In the initial form of this IBP-reduced result, some of our expressions exhibit  $1/(d-3)^2$  singularities. These divergences imply that the corresponding master integrals would be required up to  $\mathcal{O}(\epsilon^2)$ . A possible way to circumvent this is to perform a basis transformation within the IBP reduction. The idea is to exploit additional IBP relations that modify the coefficients of the master sum-integrals in such a way that the explicit  $(d-3)$  factors in the denominators are removed. In practice, this corresponds to shifting from the basketball-type basis to one involving spectacle diagrams. Although these may be somewhat more cumbersome to evaluate individually, such a transformation can simplify the overall structure of the reduction and avoid the need for higher-order  $\epsilon$ -expansions. This procedure closely mirrors the treatment in appendix D of [64].

To this end, we list the corresponding IBP basis transformation that we obtained with an in-house FORM [118] Laporta-type algorithm [102] for finite-temperature sum-integrals [103] (cf. [64] for a crosscheck):

$$\mathcal{I}_{111110} = \frac{2}{3(d-3)^2} \left[ \frac{3d^2 - 24d + 47}{(d-4)} \mathcal{I}_{210011} + 8 \mathcal{I}_{310011}^{200} \right], \quad (\text{C.31})$$

$$\begin{aligned} \mathcal{I}_{211110}^{020} = & \frac{(d-9)(d-7)(d-2)}{2(d-6)(d-5)(d-4)(d-3)^2} (\mathcal{I}_1)^2 \mathcal{I}_3 + \frac{519 - 312d + 61d^2 - 4d^3}{2(d-6)(d-5)^2(d-4)(d-3)} (\mathcal{I}_2)^2 \mathcal{I}_1 \\ & - \frac{(3d-10)(10791 - 9060d + 2806d^2 - 380d^3 + 19d^4)}{12(d-6)(d-5)(d-4)^2(d-3)^2} \mathcal{I}_{210011} + \\ & + \frac{3(d-7)}{2(d-6)(d-4)(d-3)} \mathcal{I}_{220011}^{002} - \frac{(d-9)(d-7)}{2(d-6)(d-5)(d-4)(d-3)} \mathcal{I}_{310011}^{020} + \\ & + \frac{31401 - 16707d + 2951d^2 - 173d^3}{6(d-6)(d-5)(d-4)(d-3)^2} \mathcal{I}_{310011}^{200} + \frac{512}{(d-5)(d-4)(d-3)^2} \mathcal{I}_{510011}^{600}, \end{aligned} \quad (\text{C.32})$$

$$\begin{aligned} \mathcal{I}_{31111-2} = & - \frac{60d^6 - 1381d^5 + 12352d^4 - 52890d^3 + 103142d^2 - 49577d - 60810}{3(d-6)(d-5)(d-4)(d-3)^2(d-2)(d-1)} \mathcal{I}_{210011} \\ & + \frac{2(7d^2 - 58d + 75)}{(d-6)(d-3)(d-2)(d-1)} \mathcal{I}_{220011}^{002} \end{aligned}$$

$$\begin{aligned}
& - \frac{2(8d^6 - 207d^5 + 2195d^4 - 12246d^3 + 38222d^2 - 64347d + 46743)}{(d-7)(d-6)(d-5)^2(d-3)(d-2)(d-1)} \mathcal{I}_{221000} \\
& - \frac{2(d-9)(d-7)(d+1)}{(d-6)(d-5)(d-3)(d-2)(d-1)} \mathcal{I}_{310011}^{020} \\
& - \frac{2(185d^4 - 3002d^3 + 15280d^2 - 19126d - 26841)}{3(d-6)(d-5)(d-3)^2(d-2)(d-1)} \mathcal{I}_{310011}^{200} \\
& - \frac{2(6d^7 - 166d^6 + 1971d^5 - 13028d^4 + 51730d^3 - 123276d^2 + 163349d - 92682)}{(d-7)(d-6)(d-5)(d-3)^2(d-2)(d-1)} \mathcal{I}_{311000} \\
& + \frac{16(d-5)(d-4)}{(d-2)(d-1)} \mathcal{I}_{311110}^{022} + \frac{2048(d+1)}{(d-5)(d-3)^2(d-2)(d-1)} \mathcal{I}_{510011}^{600}. \tag{C.33}
\end{aligned}$$

After applying these basis transformations, the bare correlators are compactly written as follows

$$\begin{aligned}
\Pi_{B_0 B_0}^{3\ell, (B)} &= 2g^6 \left[ (d-5)d^2(\mathcal{I}_1)^2 \mathcal{I}_3 + \frac{(d-3)(3d^3 - 27d^2 + 52d + 16)}{(d-5)(d-2)} \mathcal{I}_1(\mathcal{I}_2)^2 \right. \\
&\quad \left. + 2(d-3) \left( 2(d-1)\mathcal{I}_{210011} - (d-3)(d-1)\mathcal{I}_{111110} - 8(d-4)\mathcal{I}_{211110}^{020} \right) \right] \\
&+ 8g^4\lambda \left[ 2d(d-5)(\mathcal{I}_1)^2 \mathcal{I}_3 + \frac{(d+2)(d-3)^2}{d-2} \mathcal{I}_1(\mathcal{I}_2)^2 + 2(d-3)(3d-7)\mathcal{I}_{111110} \right] \\
&+ 32(d-3)g^2\lambda^2 \left[ \frac{d-5}{d-3} (\mathcal{I}_1)^2 \mathcal{I}_3 + \mathcal{I}_1(\mathcal{I}_2)^2 + \mathcal{I}_{210011} - \frac{d-3}{2} \mathcal{I}_{111110} \right], \tag{C.34}
\end{aligned}$$

$$\begin{aligned}
\Pi_{\phi^\dagger \phi}^{3\ell, (B)} &= g^6 \left[ (4(d-5) - d^2\xi)(\mathcal{I}_1)^2 \mathcal{I}_3 \right. \\
&\quad \left. + \left( \frac{4d^4 - 29d^3 + 43d^2 - 24d + 32}{2(d-5)(d-2)} + \frac{d\xi^2}{2} - 2(d-1)\xi \right) \mathcal{I}_1(\mathcal{I}_2)^2 \right. \\
&\quad \left. + 6(d-1)\mathcal{I}_{210011} + 4(d-2)\mathcal{I}_{111110} - 8(d-4)\mathcal{I}_{211110}^{020} + 4\mathcal{I}_{31111-2} \right] \\
&+ 4g^4\lambda \left[ d(d-2\xi)(\mathcal{I}_1)^2 \mathcal{I}_3 + \left( \frac{10d^3 - 75d^2 + 139d - 8}{2(d-5)(d-2)} - \frac{(2d-\xi)\xi}{2} \right) \mathcal{I}_1(\mathcal{I}_2)^2 \right. \\
&\quad \left. + 2(d-1)\mathcal{I}_{210011} + 4(d-1)\mathcal{I}_{111110} - 8(d-4)\mathcal{I}_{211110}^{020} \right] \\
&+ 8g^2\lambda^2 \left[ 2(2d-\xi)(\mathcal{I}_1)^2 \mathcal{I}_3 + \mathcal{I}_1(\mathcal{I}_2)^2 \left( \frac{2d^3 - 12d^2 + 3d + 36}{(d-5)(d-2)} - 2\xi \right) \right. \\
&\quad \left. + \mathcal{I}_{210011} - 7\mathcal{I}_{111110} \right] \\
&+ 32\lambda^3 \left[ 2(\mathcal{I}_1)^2 \mathcal{I}_3 + \frac{2d^2 - 14d + 17}{(d-2)(d-5)} \mathcal{I}_1(\mathcal{I}_2)^2 + \mathcal{I}_{210011} + \frac{5}{2} \mathcal{I}_{111110} \right]. \tag{C.35}
\end{aligned}$$

The remaining master integrals of mass-dimension  $\text{dim} = 2$  in eqs. (C.34) and (C.35) are

$$\text{dim} = 2, \quad \mathcal{I}_{111110}, \mathcal{I}_{211110}^{020}, \mathcal{I}_{31111-2}^{000}, \mathcal{I}_{210011}^{000}, \quad (\text{C.36})$$

and require case-by-case treatment, as done in appendix B.

## C.2. Three-loop thermal masses in the $\text{SU}(N) +$ fundamental scalar model

Our computations are straightforwardly generalized to obtain the three-loop contributions to thermal masses in a  $\text{SU}(N) +$  fundamental scalar theory. The model in 4d Euclidean spacetime is

$$\mathcal{L} = \frac{1}{4}F_{\mu\nu}^a F_{\mu\nu}^a + (D_\mu\phi)^\dagger (D_\mu\phi) + \mu^2\phi^\dagger\phi + \lambda(\phi^\dagger\phi)^2 + \mathcal{L}_{\text{gh}} + \mathcal{L}_{\text{GF}}, \quad (\text{C.37})$$

where  $\phi$  is a scalar in the fundamental representation of  $\text{SU}(N)$ ,  $F_{\mu\nu}^a = \partial_\mu A_\nu^a - \partial_\nu A_\mu^a + g f^{abc} A_\mu^b A_\nu^c$  the field-strength tensor, and  $D_\mu\phi = \partial_\mu\phi - ig T^a A_\mu^a \phi$  the covariant derivative where  $g$  is the gauge coupling.  $f^{abc}$  are the structure constants, and  $[T^a]_{ij}$  are the generators of the algebra. Finally,  $\mathcal{L}_{\text{gh}}$  is the ghost, and  $\mathcal{L}_{\text{GF}}$  the  $R_\xi$  gauge-fixing Lagrangian, which we do not display here. The latter is similar to the  $\text{U}(1)$  case (2.2), but in the background field gauge receives further contributions [80, 119]. The corresponding soft Lagrangian is similar to  $\text{U}(1)$  case (3.3), with additional group invariants appearing for general  $N$  [80].

The dimensional reduction of subsectors of this model up to  $\mathcal{O}(g^4)$  has been presented in [64, 108, 120, 121] and in `DRalgo` [122]. The relevant RG equations are also given in [122, 123], specialized to  $\text{SU}(2)$ . Here, we focus on the three-loop two-point correlators for the temporal and Lorentz scalars, which contribute to the corresponding Debye mass (3.4) and scalar thermal mass (3.5). In the following, the results are given for general  $\text{SU}(N)$ ; by setting  $N = 2$ , one recovers the results for the  $\text{SU}(2) +$  Higgs sector of the SM. Omitting now the  $(B)$  superscript to avoid the clutter of notation, the corresponding scalar and Debye masses at one-loop level are given by the bare correlators

$$\Pi_{A_0 A_0}^{1\ell} = g^2(d-1) \left( (d-1)C_A + 1 \right) \mathcal{I}_1, \quad (\text{C.38})$$

$$\Pi_{A_0 A_0}^{1\ell,(1)} = -g^2 \left[ \left( \frac{d^2 + d + 10}{6} - (d-3)\xi \right) C_A + \frac{d-4}{6} \right] \mathcal{I}_2, \quad (\text{C.39})$$

$$\Pi_{A_0 A_0}^{1\ell,(2)} = g^2 \left[ \left( \frac{2d^2 + 11d + 2}{60} - \frac{d-4}{2}\xi + \frac{d-6}{12}\xi^2 \right) C_A + \frac{d-6}{30} \right] \mathcal{I}_3, \quad (\text{C.40})$$

$$\Pi_{\phi^\dagger\phi}^{1\ell} = \left[ dg^2 C_F + 2\lambda(C_A + 1) \right] \mathcal{I}_1, \quad (\text{C.41})$$

$$\Pi_{\phi^\dagger\phi}^{1\ell,(1)} = -g^2 C_F (3 - \xi) \mathcal{I}_2, \quad (\text{C.42})$$

$$\Pi_{\phi^\dagger \phi}^{1\ell,(2)} = g^2 C_F \frac{5 - 3\xi}{3} \mathcal{I}_3. \quad (\text{C.43})$$

At two-loop level, the bare correlators read

$$\begin{aligned} \Pi_{A_0 A_0}^{2\ell} = g^4 (d-3) & \left[ C_A^2 (d-1)^2 (\xi-2) + \frac{C_A - 2C_F}{2} (d + C_A^2 (4 - 5d + 2(d-1)\xi)) \right] \mathcal{I}_1 \mathcal{I}_2 \\ & - 2g^2 \lambda (d-3) (C_A + 1) \mathcal{I}_1 \mathcal{I}_2, \end{aligned} \quad (\text{C.44})$$

$$\begin{aligned} \Pi_{A_0 A_0}^{2\ell,(1)} = g^4 & \left[ \frac{(d-3)}{(d-7)(d-5)(d-2)d} \left( C_A^2 \frac{4d^6 - 67d^5 + 385d^4 - 1033d^3 + 1459d^2 - 700d + 672}{24} \right. \right. \\ & + C_A \frac{d^5 - 18d^4 + 106d^3 - 234d^2 + 169d - 96}{6} \\ & + (C_A - 2C_F)(d-4)(d^2 - 4d - 3) \left. \right) \mathcal{I}_2^2 \\ & - C_A (d-3) \left( \left( \frac{d-4}{6} + C_A \frac{2d^3 - 5d^2 + 19d - 40}{12(d-2)} \right) \xi \right. \\ & \left. - C_A \frac{3d^2 - 13d + 16}{8(d-2)} \xi^2 \right) \mathcal{I}_2^2 \\ & + \left( C_A^2 \frac{(d-1)^2 (5d^3 - 53d^2 + 126d - 144)}{6(d-7)d} \right. \\ & + C_A \frac{6d^4 - 71d^3 + 221d^2 - 270d + 144}{6(d-7)d} - \frac{(d-6)d}{6} (C_A - 2C_F) \\ & \left. - \frac{C_A}{3} (C_A(d-1) + 1)(d-1) \left( 2(d-3)\xi - \frac{d-6}{2} \xi^2 \right) \right) \mathcal{I}_1 \mathcal{I}_3 \\ & + \frac{2}{3} g^2 \lambda (d-6) (C_A + 1) \mathcal{I}_1 \mathcal{I}_3, \end{aligned} \quad (\text{C.45})$$

$$\begin{aligned} \Pi_{\phi^\dagger \phi}^{2\ell} = g^4 C_F & \left( -(d-1)(C_A(d-1) + 1) + C_F d \xi \right) \mathcal{I}_1 \mathcal{I}_2 \\ & - 2g^2 \lambda C_F (C_A + 1) (d - \xi) \mathcal{I}_1 \mathcal{I}_2 - 4\lambda^2 (C_A + 1)^2 \mathcal{I}_1 \mathcal{I}_2, \end{aligned} \quad (\text{C.46})$$

$$\begin{aligned} \Pi_{\phi^\dagger \phi}^{2\ell,(1)} = g^4 C_F & \left[ \frac{C_A - 2C_F}{(d-7)(d-5)(d-2)d} \left( \frac{C_A^2 (19d^4 - 238d^3 + 995d^2 - 1436d - 384)}{8} \right. \right. \\ & + 2C_A (d^2 - 7d + 15) - \frac{11d^4 - 142d^3 + 575d^2 - 696d + 72}{4} \left. \right) \mathcal{I}_2^2 \\ & + \frac{C_A - 2C_F}{4} \left( 6 - \frac{C_A^2 (78 + 7(d-7)d)}{(d-5)(d-2)} \right) \xi \mathcal{I}_2^2 \end{aligned}$$

$$\begin{aligned}
& - \frac{C_A - 2C_F}{8} \left( 2 - \frac{C_A^2(28 + 3(d-7)d)}{(d-5)(d-2)} \right) \xi^2 \mathcal{I}_2^2 \\
& + \left( \frac{4(d-6)(d-1)}{(d-7)d} (C_A(d-1) + 1) + \frac{2d}{3}(5 - 3\xi)C_F \right) \mathcal{I}_1 \mathcal{I}_3 \Big] \\
& + \frac{4}{3} g^2 \lambda C_F (C_A + 1)(5 - 3\xi) \mathcal{I}_1 \mathcal{I}_3 + 12\lambda^2 (C_A + 1) \frac{(d-3)(d-4)}{(d-7)(d-5)(d-2)d} \mathcal{I}_2^2. \quad (C.47)
\end{aligned}$$

The Debye mass is computed in the background field gauge [124]. We have crosschecked that the pure gauge contributions agree with [64] when adapting our gauge parameter convention via  $\xi \rightarrow 1 - \xi_{[64]}$ .

The three-loop part of two-point bare correlators for the temporal and Lorentz scalars contribute to the corresponding Debye mass (3.4) and scalar thermal mass (3.5). They are given by

$$\begin{aligned}
\Pi_{A_0 A_0}^{3\ell} = g^6 & \left[ \left( \frac{(d-1)^2(d^3 + 40d^2 - 347d + 594)}{12} C_A^3 + \frac{2d^4 + 81d^3 - 789d^2 + 1882d - 1188}{12} C_A^2 \right. \right. \\
& + \frac{d^3 + 40d^2 - 347d + 594}{12} C_A - \frac{(2C_A^2 - 1)(d-5)d^2}{4C_A^2} \\
& + \frac{(d-1)^2}{12} C_A (C_A(d-1) + 1)^2 ((d-6)\xi - 2d)\xi \Big) (\mathcal{I}_1)^2 \mathcal{I}_3 \\
& + (d-3) \left( \frac{(d-1)^2(19d^3 - 180d^2 + 421d - 60)}{8(d-5)(d-2)} C_A^3 \right. \\
& + \frac{31d^4 - 301d^3 + 827d^2 - 589d + 72}{8(d-5)(d-2)} C_A^2 + \frac{d^3 - 7d^2 + 9d - 3}{2(d-5)(d-2)} C_A \\
& - \frac{3d^4 - 26d^3 + 54d^2 - 3d - 8}{2(d-5)(d-2)} - \frac{d^3 - 8d^2 + 11d + 8}{2(d-5)(d-2)C_A} + \frac{(d-6)d}{4(d-2)C_A^2} \\
& + \frac{(d-1)^2}{d-2} \left( \frac{3d^2 - 13d + 16}{8} \xi^2 - \frac{7d^2 - 39d + 48}{4} \xi \right) C_A^3 \\
& + \frac{1}{d-2} \left( \frac{3d^3 - 16d^2 + 29d - 16}{8} \xi^2 - \frac{9d^3 - 56d^2 + 99d - 48}{4} \xi \right) C_A^2 \\
& \left. \left. + \frac{(d-3)d}{2} \xi \right) \mathcal{I}_1 (\mathcal{I}_2)^2 \right. \\
& - (d-3) \left( 3(d-1)C_A^2 + \frac{3}{2}C_A + \frac{4d-1}{2} - \frac{3}{2} \frac{1}{C_A} - \frac{2d+1}{2C_A^2} \right) \mathcal{I}_{210011} \\
& - (d-3) \left( \frac{(d-1)^2(7d-13)}{4} C_A^3 + \frac{(d-1)(d+3)}{2} C_A^2 + \frac{d+3}{4} C_A \right. \\
& \left. - \frac{5(d^2 - 3d + 1)}{2} - \frac{3d-5}{4C_A} + \frac{2d^2 - 11d + 11}{4C_A^2} \right) \mathcal{I}_{111110} \\
& - 8(d-4)(d-3)(C_A(d-1) + 1)(C_A^2(d-1) + C_F) \mathcal{I}_{211110}^{020}
\end{aligned}$$

$$\begin{aligned}
& - \frac{(d-7)(d-3)}{2} C_A (C_A(d-1) + 1)^2 \mathcal{I}_{31111-2} \Big] \\
& + (C_A + 1)(C_A - 2C_F) g^4 \lambda \Big[ 2d(d-5)d_A (\mathcal{I}_1)^2 \mathcal{I}_3 \\
& + \left( \frac{(d-3)^2(C_A^2(5d-2) - (d+2))}{d-2} - 2C_A^2(d-3)^2 \xi \right) \mathcal{I}_1 (\mathcal{I}_2)^2 \\
& + (d-3)(3d-7) \frac{C_A^2 + 2(C_A - 1)}{C_A + 1} \mathcal{I}_{111110} \Big] \\
& + 4(d-3) g^2 \lambda^2 (C_A + 1) \Big[ (C_A + 1) \frac{d-5}{d-3} (\mathcal{I}_1)^2 \mathcal{I}_3 + (C_A + 1) \mathcal{I}_1 (\mathcal{I}_2)^2 \\
& + 2\mathcal{I}_{210011} - (d-3) \mathcal{I}_{111110} \Big], \tag{C.48}
\end{aligned}$$

$$\begin{aligned}
\Pi_{\phi^\dagger \phi}^{3\ell} = & g^6 C_F \Big[ ((C_A(d-1) + 1)^2(d-5) - d^2 C_F^2 \xi) (\mathcal{I}_1)^2 \mathcal{I}_3 \\
& + \left( \frac{d(3d^2 - 25d + 36)}{8C_A^2(d-5)(d-2)} - \frac{9d^3 - 123d^2 + 252d - 64}{16(d-5)(d-2)} \right. \\
& \left. - \frac{d^4 - 8d^2 + 17d^2 - 15d + 12}{2C_A(d-5)(d-2)} + \frac{C_A(3d^4 - 26d^3 + 63d^2 - 37d + 4)}{2(d-5)(d-2)} \right. \\
& \left. + \frac{C_A^2 d(16d^4 - 160d^3 + 515d^2 - 585d + 228)}{16(d-5)(d-2)} \right. \\
& \left. - C_F \left( (d-1) + C_A \frac{4d^4 - 35d^3 + 93d^2 - 90d + 40}{4(d-5)(d-2)} \right) \xi \right. \\
& \left. - dC_F \left( \frac{1}{4C_A} - C_A \frac{3d^2 - 21d + 28}{8(d-5)(d-2)} \right) \xi^2 \right) \mathcal{I}_1 (\mathcal{I}_2)^2 \\
& - \left( \frac{d-1}{2} C_A^2 + \frac{4d-1}{4} C_A + \frac{4d-7}{4C_A} - \frac{2d+1}{4C_A^2} + \frac{3}{4} \right) \mathcal{I}_{210011} \\
& - \left( \frac{d^2 - 11d + 1}{2} C_A^2 + \frac{6d+5}{4} C_A + \frac{7-4d}{4C_A^2} - 5d + 4 \right) \mathcal{I}_{111110} \\
& - 2(d-4)(C_A - 2C_F)(C_A^2(2d-1) - 1)(C_A(d-1) + 1) \mathcal{I}_{211110}^{020} \\
& + (C_A(d-1) + 1)^2 \mathcal{I}_{31111-2} \Big] \\
& + g^4 \lambda d_A (C_A + 1) \Big[ 2d(d-2\xi) \frac{C_F^2}{d_A} (\mathcal{I}_1)^2 \mathcal{I}_3 \\
& + \left( \frac{8d^4 - 68d^3 + 159d^2 - 89d + 52}{8(d-5)(d-2)} \right. \\
& \left. + \frac{2d^3 - 16d^2 + 32d - 11}{C_A(d-5)(d-2)} - \frac{4d^3 - 22d^2 + 22d + 72}{8C_A^2(d-5)(d-2)} \right)
\end{aligned}$$

$$\begin{aligned}
& + \left( \frac{2d}{C_A^2} - \frac{2d^3 - 13d^2 + 13d + 18}{(d-5)(d-2)} \right) \frac{\xi}{4} - \left( \frac{1}{C_A^2} - \frac{3d^2 - 21d + 28}{2(d-5)(d-2)} \right) \frac{\xi^2}{4} \right) \mathcal{I}_1(\mathcal{I}_2)^2 \\
& - \frac{2d+1+3C_A+2C_A^2(d-1)}{2C_A^2} \mathcal{I}_{210011} \\
& - \frac{C_A - 2C_F}{2C_A(C_A + 1)} (2(2d-1) - C_A(4(d-3) + 13C_A - 2C_A^2(d-9))) \mathcal{I}_{111110} \\
& - 4(d-4)(C_A - 2C_F)(C_A(d-1) + 1) \mathcal{I}_{211110}^{020} \Big] \\
& + 2g^2 \lambda^2 d_A (C_A + 1) (C_A - 2C_F) \left[ (C_A + 1)(2d - \xi) (\mathcal{I}_1)^2 \mathcal{I}_3 \right. \\
& + \left( \frac{d^3 - 6d^2 + 18 + C_A(d-3)(d^2 - 3d - 6)}{(d-5)(d-2)} - (C_A + 1)\xi \right) \mathcal{I}_1(\mathcal{I}_2)^2 \\
& \left. + \mathcal{I}_{210011} - 7\mathcal{I}_{111110} \right] \\
& + 8\lambda^3 (C_A + 1)^2 \left[ (C_A + 1)(\mathcal{I}_1)^2 \mathcal{I}_3 + \left( C_A + \frac{d^2 - 7d + 7}{(d-5)(d-2)} \right) \mathcal{I}_1(\mathcal{I}_2)^2 \right. \\
& \left. + \mathcal{I}_{210011} + \frac{C_A + 4}{C_A + 1} \mathcal{I}_{111110} \right]. \tag{C.49}
\end{aligned}$$

In the expressions above,  $C_A = N$  and  $C_F = (N^2 - 1)/(2N)$  are the Casimirs of the adjoint and fundamental representations of  $SU(N)$ , respectively, and  $d_A = N^2 - 1$  is the dimension of the adjoint representation.

### C.3. On the mismatch in the master integral $\mathcal{I}_{31111-2}$

In our derivation of the full  $\mathcal{O}(g^6)$  dimensional reduction of the Abelian Higgs model, we find that the renormalized scalar mass  $\mu_3^2$  contains a leftover  $1/\epsilon$  pole that is not canceled upon the introduction of the corresponding 3d counterterm  $\delta\mu_3^2$ . This leftover pole,

$$\mu_3^2 = -\frac{2}{9(4\pi)^4 \epsilon} g^6 T^2 + \mathcal{O}(\epsilon^0), \tag{C.50}$$

arises at three-loop order, while all other poles, involving different powers of  $g$  or  $\lambda$  are absent. From eq. (C.35), we see that there is a sum-integral,  $\mathcal{I}_{31111-2}$ , that is unique to the  $g^6$  contribution to the three-loop scalar correlator. Given the self-consistency of our computation in all other terms, we identify the  $\epsilon$ -expansion of this sum-integral (eq. (B.8)) as a potential source of error. Indeed, if we modify this expression by  $\delta\mathcal{I}_{31111-2}$  (see eq. (3.10)), this leftover pole is canceled for  $X = -2/5$  without spoiling any other consistency check.

To further examine this issue, we explore the  $SU(2) +$  fundamental scalar theory, employing the results in appendix C.2 for  $N = 2$ . In this model, the two-loop counterterm for the 3d

scalar mass is known [78, 117], *viz.*

$$\delta\mu_3^2 = -\frac{1}{4(4\pi)^2}\frac{1}{\epsilon}\left(\frac{39}{16}g_3^4 + 12h_3g_3^2 - 6h_3^2 + 9\lambda_3g_3^2 - 12\lambda_3^2\right), \quad (\text{C.51})$$

where the 3d soft scale couplings are the same as those in eq. (3.3), upon replacing the fields in U(1) representations with the corresponding ones in the SU(2) case. Its SU( $N$ ) generalization,

$$\begin{aligned} \delta\mu_3^2 = -\frac{1}{(4\pi)^2}\frac{1}{\epsilon}\left[ C_{\text{F}}\frac{3C_{\text{A}}^2 - C_{\text{A}} + 3}{8C_{\text{A}}}g_3^4 + (C_{\text{A}} + 1)(C_{\text{F}}\lambda_3g_3^2 - \lambda_3^2) \right. \\ \left. + C_{\text{F}}C_{\text{A}}(C_{\text{A}}h_3 + 2h_{3,2})g_3^2 - C_{\text{F}}\left(C_{\text{A}}h_3^2 + 4h_3h_{3,2} - 2(C_{\text{A}} - 4C_{\text{F}})h_{3,2}^2\right)\right], \end{aligned} \quad (\text{C.52})$$

features a second scalar-gauge coupling,  $h_{3,2}$ , that appears in the SU( $N$ ) case besides  $h_3$ .<sup>7</sup> To see this, we decompose the product of generators as  $T^aT^b = \frac{1}{2}\{T^a, T^b\} + \frac{1}{2}[T^a, T^b]$ , and note that the antisymmetric part vanishes since  $A_0^aA_0^b$  is symmetric under interchange of indices. Then, by using  $\{T^a, T^b\} = \frac{1}{N}\delta^{ab} + d^{abc}T^c$ , we see that in general the SU( $N$ ) counterpart of the 3d soft-scale Lagrangian (C.1) contains the two distinct scalar-gauge interaction terms

$$\mathcal{L}_{\text{soft}} \supset h_3\phi^\dagger\phi A_0^aA_0^a + h_{3,2}\phi^\dagger T^c\phi d^{abc}A_0^aA_0^b. \quad (\text{C.53})$$

While in general SU( $N$ ) the symmetric structure constants  $d^{abc}$  are non-vanishing, for SU(2) they identically vanish and therefore  $h_{3,2}$  does not contribute.

The mismatch in the  $\mathcal{O}(\epsilon^{-1})$  coefficient of  $\mathcal{I}_{31111-2}$  affects only scalar mass renormalization. While this integral appears in the pure gauge Debye mass in eq. (C.48) (cf. [64]), the corresponding term is rendered finite by an explicit  $(d-3)$  factor. In contrast, for scalar mass renormalization in eq. (C.49), the prefactor is not lifted to  $\mathcal{O}(\epsilon^0)$ , leading to the leftover pole

$$\mu_3^2\Big|_{\text{SU}(2)} = -\frac{25}{24(4\pi)^4\epsilon}g^6T^2 + \mathcal{O}(\epsilon^0), \quad (\text{C.54})$$

which is neatly canceled by  $\delta\mathcal{I}_{31111-2}$  with the same  $X = -2/5$ .

In the original derivation of the three-loop Debye mass [64], errors in the  $1/\epsilon$  coefficient of  $\mathcal{I}_{31111-2}$  were masked as finite contributions due to the multiplicative  $(d-3)$  factor and could not be verified by renormalization. Our finding thus warrants re-evaluation of this standard result.

## References

[1] G. M. Harry, P. Fritschel, D. A. Shaddock, W. Folkner, and E. S. Phinney, *Laser interferometry for the big bang observer*, Class. Quant. Grav. **23** (2006) 4887.

---

<sup>7</sup>Similarly, the temporal quartic couplings are linearly dependent only for  $N \leq 3$  [80].

[2] S. Kawamura *et al.*, *The Japanese space gravitational wave antenna DECIGO*, Class. Quant. Grav. **23** (2006) S125.

[3] W.-H. Ruan, Z.-K. Guo, R.-G. Cai, and Y.-Z. Zhang, *Taiji program: Gravitational-wave sources*, Int. J. Mod. Phys. A **35** (2020) 2050075 [1807.09495].

[4] **LIGO Scientific** Collaboration, J. Aasi *et al.*, *Advanced LIGO*, Class. Quant. Grav. **32** (2015) 074001 [1411.4547].

[5] C. Caprini *et al.*, *Detecting gravitational waves from cosmological phase transitions with LISA: an update*, JCAP **03** (2020) 024 [1910.13125].

[6] **NANOGrav** Collaboration, Z. Arzoumanian *et al.*, *The NANOGrav 12.5 yr Data Set: Search for an Isotropic Stochastic Gravitational-wave Background*, Astrophys. J. Lett. **905** (2020) L34 [2009.04496].

[7] K. Kajantie, M. Laine, K. Rummukainen, and M. E. Shaposhnikov, *Is there a hot electroweak phase transition at  $m_H \gtrsim m_W$ ?*, Phys. Rev. Lett. **77** (1996) 2887 [hep-ph/9605288].

[8] M. Gurtler, E.-M. Ilgenfritz, and A. Schiller, *Where the electroweak phase transition ends*, Phys. Rev. D **56** (1997) 3888 [hep-lat/9704013].

[9] F. Csikor, Z. Fodor, and J. Heitger, *Endpoint of the hot electroweak phase transition*, Phys. Rev. Lett. **82** (1999) 21 [hep-ph/9809291].

[10] E. Braaten and A. Nieto, *Effective field theory approach to high temperature thermodynamics*, Phys. Rev. D **51** (1995) 6990 [hep-ph/9501375].

[11] E. Braaten, *Solution to the perturbative infrared catastrophe of hot gauge theories*, Phys. Rev. Lett. **74** (1995) 2164 [hep-ph/9409434].

[12] E. Braaten and A. Nieto, *Free energy of QCD at high temperature*, Phys. Rev. D **53** (1996) 3421 [hep-ph/9510408].

[13] K. Kajantie, M. Laine, K. Rummukainen, and M. E. Shaposhnikov, *3-D  $SU(N) + \text{adjoint Higgs theory and finite temperature QCD}$* , Nucl. Phys. B **503** (1997) 357 [hep-ph/9704416].

[14] M. Laine, P. Schicho, and Y. Schröder, *A QCD Debye mass in a broad temperature range*, Phys. Rev. D **101** (2020) 023532 [1911.09123].

[15] M. Laine, P. Schicho, and Y. Schröder, *Soft thermal contributions to 3-loop gauge coupling*, JHEP **05** (2018) 037 [1803.08689].

[16] J. Ghiglieri, G. D. Moore, P. Schicho, and N. Schluesser, *The force-force-correlator in hot QCD perturbatively and from the lattice*, JHEP **02** (2022) 058 [2112.01407].

[17] P. Navarrete and Y. Schröder, *The  $g^6$  pressure of hot Yang-Mills theory: canonical form of the integrand*, JHEP **11** (2024) 037 [2408.15830].

[18] T. Gorda, P. Navarrete, R. Paatelainen, L. Sandbete, and K. Seppänen, *A new approach to determine the thermodynamics of deconfined matter to high accuracy*, [2511.09627].

- [19] T. Matsubara, *A New approach to quantum statistical mechanics*, Prog. Theor. Phys. **14** (1955) 351.
- [20] P. H. Ginsparg, *First Order and Second Order Phase Transitions in Gauge Theories at Finite Temperature*, Nucl. Phys. B **170** (1980) 388.
- [21] T. Appelquist and R. D. Pisarski, *High-Temperature Yang-Mills Theories and Three-Dimensional Quantum Chromodynamics*, Phys. Rev. D **23** (1981) 2305.
- [22] T. Brauner, T. V. I. Tenkanen, A. Tranberg, A. Vuorinen, and D. J. Weir, *Dimensional reduction of the Standard Model coupled to a new singlet scalar field*, JHEP **03** (2017) 007 [1609.06230].
- [23] J. O. Andersen, T. Gorda, A. Helset, *et al.*, *Nonperturbative Analysis of the Electroweak Phase Transition in the Two Higgs Doublet Model*, Phys. Rev. Lett. **121** (2018) 191802 [1711.09849].
- [24] L. Niemi, H. H. Patel, M. J. Ramsey-Musolf, T. V. I. Tenkanen, and D. J. Weir, *Electroweak phase transition in the real triplet extension of the SM: Dimensional reduction*, Phys. Rev. D **100** (2019) 035002 [1802.10500].
- [25] T. Gorda, A. Helset, L. Niemi, T. V. I. Tenkanen, and D. J. Weir, *Three-dimensional effective theories for the two Higgs doublet model at high temperature*, JHEP **02** (2019) 081 [1802.05056].
- [26] K. Kainulainen, V. Keus, L. Niemi, K. Rummukainen, T. V. I. Tenkanen, and V. Vaskonen, *On the validity of perturbative studies of the electroweak phase transition in the Two Higgs Doublet model*, JHEP **06** (2019) 075 [1904.01329].
- [27] D. Croon, O. Gould, P. Schicho, T. V. I. Tenkanen, and G. White, *Theoretical uncertainties for cosmological first-order phase transitions*, JHEP **04** (2021) 055 [2009.10080].
- [28] O. Gould, J. Kozaczuk, L. Niemi, M. J. Ramsey-Musolf, T. V. I. Tenkanen, and D. J. Weir, *Non-perturbative analysis of the gravitational waves from a first-order electroweak phase transition*, Phys. Rev. D **100** (2019) 115024 [1903.11604].
- [29] L. Niemi, M. J. Ramsey-Musolf, T. V. I. Tenkanen, and D. J. Weir, *Thermodynamics of a Two-Step Electroweak Phase Transition*, Phys. Rev. Lett. **126** (2021) 171802 [2005.11332].
- [30] O. Gould and J. Hirvonen, *Effective field theory approach to thermal bubble nucleation*, Phys. Rev. D **104** (2021) 096015 [2108.04377].
- [31] O. Gould, *Real scalar phase transitions: a nonperturbative analysis*, JHEP **04** (2021) 057 [2101.05528].
- [32] P. M. Schicho, T. V. I. Tenkanen, and J. Österman, *Robust approach to thermal resummation: Standard Model meets a singlet*, JHEP **06** (2021) 130 [2102.11145].
- [33] L. Niemi, P. Schicho, and T. V. I. Tenkanen, *Singlet-assisted electroweak phase transition at two loops*, Phys. Rev. D **103** (2021) 115035 [2103.07467].
- [34] J. E. Camargo-Molina, R. Enberg, and J. Löfgren, *A new perspective on the electroweak phase transition in the Standard Model Effective Field Theory*, JHEP **10** (2021) 127 [2103.14022].
- [35] L. Niemi, K. Rummukainen, R. Seppä, and D. J. Weir, *Infrared physics of the 3D  $SU(2)$  adjoint Higgs model at the crossover transition*, JHEP **02** (2023) 212 [2206.14487].

[36] A. Ekstedt, *Convergence of the nucleation rate for first-order phase transitions*, Phys. Rev. D **106** (2022) 095026 [[2205.05145](#)].

[37] O. Gould, S. Güyer, and K. Rummukainen, *First-order electroweak phase transitions: A non-perturbative update*, Phys. Rev. D **106** (2022) 114507 [[2205.07238](#)].

[38] A. Ekstedt, O. Gould, and J. Löfgren, *Radiative first-order phase transitions to next-to-next-to-leading order*, Phys. Rev. D **106** (2022) 036012 [[2205.07241](#)].

[39] S. Biondini, P. Schicho, and T. V. I. Tenkanen, *Strong electroweak phase transition in t-channel simplified dark matter models*, JCAP **10** (2022) 044 [[2207.12207](#)].

[40] P. Schicho, T. V. I. Tenkanen, and G. White, *Combining thermal resummation and gauge invariance for electroweak phase transition*, JHEP **11** (2022) 047 [[2203.04284](#)].

[41] J. Löfgren, M. J. Ramsey-Musolf, P. Schicho, and T. V. I. Tenkanen, *Nucleation at Finite Temperature: A Gauge-Invariant Perturbative Framework*, Phys. Rev. Lett. **130** (2023) 251801 [[2112.05472](#)].

[42] O. Gould and C. Xie, *Higher orders for cosmological phase transitions: a global study in a Yukawa model*, JHEP **12** (2023) 049 [[2310.02308](#)].

[43] M. Kierkla, B. Swiezewska, T. V. I. Tenkanen, and J. van de Vis, *Gravitational waves from supercooled phase transitions: dimensional transmutation meets dimensional reduction*, JHEP **02** (2024) 234 [[2312.12413](#)].

[44] G. Aarts *et al.*, *Phase Transitions in Particle Physics: Results and Perspectives from Lattice Quantum Chromo-Dynamics*, Prog. Part. Nucl. Phys. **133** (2023) 104070 [[2301.04382](#)].

[45] L. Niemi, M. J. Ramsey-Musolf, and G. Xia, *Nonperturbative study of the electroweak phase transition in the real scalar singlet extended standard model*, Phys. Rev. D **110** (2024) 115016 [[2405.01191](#)].

[46] M. Chala, J. C. Criado, L. Gil, and J. L. Miras, *Higher-order-operator corrections to phase-transition parameters in dimensional reduction*, JHEP **10** (2024) 025 [[2406.02667](#)].

[47] R. Qin and L. Bian, *First-order electroweak phase transition at finite density*, JHEP **08** (2024) 157 [[2407.01981](#)].

[48] O. Gould and P. M. Saffin, *Perturbative gravitational wave predictions for the real-scalar extended Standard Model*, JHEP **03** (2025) 105 [[2411.08951](#)].

[49] J. Chakrabortty and S. Mohanty, *One Loop Thermal Effective Action*, Nucl. Phys. B **1020** (2025) 117165 [[2411.14146](#)].

[50] L. Niemi and T. V. I. Tenkanen, *Investigating two-loop effects for first-order electroweak phase transitions*, Phys. Rev. D **111** (2025) 075034 [[2408.15912](#)].

[51] M. Kierkla, P. Schicho, B. Swiezewska, T. V. I. Tenkanen, and J. van de Vis, *Finite-temperature bubble nucleation with shifting scale hierarchies*, JHEP **07** (2025) 153 [[2503.13597](#)].

[52] A. Bhatnagar, D. Croon, and P. Schicho, *Interpreting the 95 GeV resonance in the Two Higgs Doublet Model: Implications for the Electroweak Phase Transition*, [[2506.20716](#)].

[53] F. Bernardo, P. Klose, P. Schicho, and T. V. I. Tenkanen, *Higher-dimensional operators at finite temperature affect gravitational-wave predictions*, JHEP **08** (2025) 109 [2503.18904].

[54] M. Chala and G. Guedes, *The high-temperature limit of the SM(EFT)*, JHEP **07** (2025) 085 [2503.20016].

[55] Y. Zhu, J. Liu, R. Qin, and L. Bian, *Theoretical uncertainties in first-order electroweak phase transitions*, Phys. Rev. D **112** (2025) 015018 [2503.19566].

[56] M. Chala, L. Gil, and Z. Ren, *Phase transitions in dimensional reduction up to three loops*, Chin. Phys. **49** (2025) 123105 [2505.14335].

[57] X.-X. Li, M. J. Ramsey-Musolf, T. V. I. Tenkanen, and Y. Wu, *An Effective Sphaleron Awakens*, [2506.01585].

[58] J. Annala, K. Rummukainen, and T. V. I. Tenkanen, *Nonperturbative determination of the sphaleron rate for first-order phase transitions*, Phys. Rev. D **113** (2026) 016014 [2506.04939].

[59] P. Navarrete, R. Paatelainen, K. Seppänen, and T. V. I. Tenkanen, *Cosmological phase transitions without high-temperature expansions*, JHEP **01** (2026) 113 [2507.07014].

[60] M. Chala, M. C. Fiore, and L. Gil, *Hot news on the phase-structure of the SMEFT*, [2507.16905].

[61] M. Chala, A. Dashko, and G. Guedes, *Running Couplings in High-Temperature Effective Field Theory*, [2510.26878].

[62] T. Biekötter, A. Dashko, M. Löschner, and G. Weiglein, *Perturbative aspects of the electroweak phase transition with a complex singlet and implications for gravitational wave predictions*, [2511.14831].

[63] A. Ekstedt, P. Schicho, and T. V. I. Tenkanen, *Cosmological phase transitions at three loops: The final verdict on perturbation theory*, Phys. Rev. D **110** (2024) 096006 [2405.18349].

[64] I. Ghisoiu, J. Moller, and Y. Schröder, *Debye screening mass of hot Yang-Mills theory to three-loop order*, JHEP **11** (2015) 121 [1509.08727].

[65] J. Jaeckel, V. V. Khoze, and M. Spannowsky, *Hearing the signal of dark sectors with gravitational wave detectors*, Phys. Rev. D **94** (2016) 103519 [1602.03901].

[66] A. Addazi and A. Marciano, *Gravitational waves from dark first order phase transitions and dark photons*, Chin. Phys. C **42** (2018) 023107 [1703.03248].

[67] D. Croon, V. Sanz, and G. White, *Model Discrimination in Gravitational Wave spectra from Dark Phase Transitions*, JHEP **08** (2018) 203 [1806.02332].

[68] M. Breitbach, J. Kopp, E. Madge, T. Opferkuch, and P. Schwaller, *Dark, Cold, and Noisy: Constraining Secluded Hidden Sectors with Gravitational Waves*, JCAP **07** (2019) 007 [1811.11175].

[69] M. Christiansen, E. Madge, C. Puchades-Ibáñez, M. E. Ramirez-Quezada, and P. Schwaller, *Beyond the Daisy Chain: Running and the 3D EFT View of Supercooled Phase Transitions*, [2511.02910].

[70] B. i. Halperin, T. C. Lubensky, and S.-k. Ma, *First order phase transitions in superconductors and smectic A liquid crystals*, Phys. Rev. Lett. **32** (1974) 292.

[71] C. Dasgupta and B. I. Halperin, *Phase Transition in a Lattice Model of Superconductivity*, Phys. Rev. Lett. **47** (1981) 1556.

[72] K. Kajantie, M. Laine, T. Neuhaus, J. Peisa, A. Rajantie, and K. Rummukainen, *Vortex tension as an order parameter in three-dimensional  $U(1) + \text{Higgs}$  theory*, Nucl. Phys. B **546** (1999) 351 [[hep-ph/9809334](#)].

[73] M. Lewicki, P. Toczek, and V. Vaskonen, *Black holes and gravitational waves from phase transitions in realistic models*, Phys. Dark Univ. **50** (2025) 102075 [[2412.10366](#)].

[74] G. Franciolini, Y. Gouttenoire, and R. Jinno, *Curvature Perturbations from First-Order Phase Transitions: Implications to Black Holes and Gravitational Waves*, [[2503.01962](#)].

[75] M. Kierkla, N. Ramberg, P. Schicho, and D. Schmitt, *Theoretical uncertainties for primordial black holes from cosmological phase transitions*, [[2506.15496](#)].

[76] O. Gould and T. V. I. Tenkanen, *Perturbative effective field theory expansions for cosmological phase transitions*, JHEP **01** (2024) 048 [[2309.01672](#)].

[77] A. D. Linde, *Infrared Problem in Thermodynamics of the Yang-Mills Gas*, Phys. Lett. B **96** (1980) 289.

[78] K. Kajantie, M. Laine, K. Rummukainen, and M. E. Shaposhnikov, *Generic rules for high temperature dimensional reduction and their application to the standard model*, Nucl. Phys. B **458** (1996) 90 [[hep-ph/9508379](#)].

[79] P. M. Stevenson, *Optimized Perturbation Theory*, Phys. Rev. D **23** (1981) 2916.

[80] M. Laine and Y. Schröder, *Two-loop QCD gauge coupling at high temperatures*, JHEP **03** (2005) 067 [[hep-ph/0503061](#)].

[81] I. Ghisoiu and Y. Schröder, *A New Method for Taming Tensor Sum-Integrals*, JHEP **11** (2012) 010 [[1208.0284](#)].

[82] M. Chala, J. López Miras, J. Santiago, and F. Vilches, *Efficient on-shell matching*, SciPost Phys. **18** (2025) 185 [[2411.12798](#)].

[83] P. B. Arnold and O. Espinosa, *The Effective potential and first order phase transitions: Beyond leading-order*, Phys. Rev. D **47** (1993) 3546 [[hep-ph/9212235](#)].

[84] E. Camargo-Molina, R. Enberg, and J. Löfgren, *A catalog of first-order electroweak phase transitions in the Standard Model Effective Field Theory*, JHEP **08** (2025) 113 [[2410.23210](#)].

[85] J. Hirvonen, J. Löfgren, M. J. Ramsey-Musolf, P. Schicho, and T. V. I. Tenkanen, *Computing the gauge-invariant bubble nucleation rate in finite temperature effective field theory*, JHEP **07** (2022) 135 [[2112.08912](#)].

[86] K. Kajantie, M. Laine, K. Rummukainen, and M. E. Shaposhnikov, *The Electroweak phase transition: A Nonperturbative analysis*, Nucl. Phys. B **466** (1996) 189 [[hep-lat/9510020](#)].

[87] K. Farakos, K. Kajantie, K. Rummukainen, and M. E. Shaposhnikov, *3-d physics and the electroweak phase transition: A Framework for lattice Monte Carlo analysis*, Nucl. Phys. B **442** (1995) 317 [[hep-lat/9412091](#)].

[88] H. Kleinert and W. Miller, *Renormalization of Charge in Villain Lattice Gauge Theory*, Phys. Rev. Lett. **56** (1986) 11.

[89] S. Mo, J. Hove, and A. Sudbo, *The Order of the metal to superconductor transition*, Phys. Rev. B **65** (2002) 104501 [[cond-mat/0109260](#)].

[90] K. Jansen, J. Jersak, C. B. Lang, T. Neuhaus, and G. Vones, *Phase Structure of  $U(1)$  Gauge - Higgs Theory on  $D = 4$  Lattices*, Phys. Lett. B **155** (1985) 268.

[91] H. Kleinert, *Tricritical Ratio of Length Scales in the  $D = 4$  Abelian Higgs Model*, Phys. Rev. Lett. **56** (1986) 1441.

[92] S. R. Coleman and E. J. Weinberg, *Radiative Corrections as the Origin of Spontaneous Symmetry Breaking*, Phys. Rev. D **7** (1973) 1888.

[93] S. Pascoli, S. Rosauro-Alcaraz, and M. Zandi, *Cosmological phase transitions: from particle physics to gravitational waves, semi-analytically*, [[2602.02829](#)].

[94] M. Lewicki, P. Toczek, and V. Vaskonen, *Primordial black holes from strong first-order phase transitions*, JHEP **09** (2023) 092 [[2305.04924](#)].

[95] B. Carr, A. J. Iovino, G. Perna, V. Vaskonen, and H. Veermäe, *Primordial black holes: constraints, potential evidence and prospects*, [[2601.06024](#)].

[96] I. Ghisoiu and Y. Schröder, *A new three-loop sum-integral of mass dimension two*, JHEP **09** (2012) 016 [[1207.6214](#)].

[97] D. Curtin, J. Roy, and G. White, *Gravitational waves and tadpole resummation: Efficient and easy convergence of finite temperature QFT*, Phys. Rev. D **109** (2024) 116001 [[2211.08218](#)].

[98] J. C. Collins and J. A. M. Verma, *Axodraw Version 2*, [[1606.01177](#)].

[99] M. Laine and A. Vuorinen, *Basics of Thermal Field Theory*, vol. 925. Springer, 2016, [[1701.01554](#)].

[100] A. I. Davydychev, P. Navarrete, and Y. Schröder, *Factorizing two-loop vacuum sum-integrals*, JHEP **02** (2024) 104 [[2312.17367](#)].

[101] A. I. Davydychev and Y. Schröder, *Recursion-free solution for two-loop vacuum integrals with “collinear” masses*, JHEP **12** (2022) 047 [[2210.10593](#)].

[102] S. Laporta, *High-precision calculation of multiloop Feynman integrals by difference equations*, Int. J. Mod. Phys. A **15** (2000) 5087 [[hep-ph/0102033](#)].

[103] M. Nishimura and Y. Schröder, *IBP methods at finite temperature*, JHEP **09** (2012) 051 [[1207.4042](#)].

[104] P. Schicho, *Multi-loop investigations of strong interactions at high temperatures*, PhD thesis, U. Bern, 2020

[105] A. V. Smirnov and A. V. Petukhov, *The Number of Master Integrals is Finite*, Lett. Math. Phys. **97** (2011) 37 [[1004.4199](#)].

[106] P. B. Arnold and C.-x. Zhai, *The Three loop free energy for high temperature QED and QCD with fermions*, Phys. Rev. D **51** (1995) 1906 [[hep-ph/9410360](#)].

[107] P. B. Arnold and C.-X. Zhai, *The Three loop free energy for pure gauge QCD*, Phys. Rev. D **50** (1994) 7603 [[hep-ph/9408276](#)].

[108] I. Ghisoiu, *Three-loop Debye mass and effective coupling in thermal QCD*, PhD thesis, U. Bielefeld (main), 2013

[109] S. Catani, T. Gleisberg, F. Krauss, G. Rodrigo, and J.-C. Winter, *From loops to trees by-passing Feynman's theorem*, JHEP **09** (2008) 065 [[0804.3170](#)].

[110] K. Seppänen, *Quark Matter Thermodynamics from High-Order Perturbative QCD*, PhD thesis, Helsinki U., 2025

[111] J. Moller and Y. Schröder, *Three-loop matching coefficients for hot QCD: Reduction and gauge independence*, JHEP **08** (2012) 025 [[1207.1309](#)].

[112] A. Gynther, M. Laine, Y. Schröder, C. Torrero, and A. Vuorinen, *Four-loop pressure of massless  $O(N)$  scalar field theory*, JHEP **04** (2007) 094 [[hep-ph/0703307](#)].

[113] J. Moller and Y. Schröder, *Open problems in hot QCD*, Nucl. Phys. B Proc. Suppl. **205-206** (2010) 218 [[1007.1223](#)].

[114] J. O. Andersen and L. Kyllingstad, *Four-loop Screened Perturbation Theory*, Phys. Rev. D **78** (2008) 076008 [[0805.4478](#)].

[115] Y. Schröder, *A fresh look on three-loop sum-integrals*, JHEP **08** (2012) 095 [[1207.5666](#)].

[116] K. Farakos, K. Kajantie, K. Rummukainen, and M. E. Shaposhnikov, *3-D physics and the electroweak phase transition: Perturbation theory*, Nucl. Phys. B **425** (1994) 67 [[hep-ph/9404201](#)].

[117] M. Laine, *Exact relation of lattice and continuum parameters in three-dimensional  $SU(2)$  + Higgs theories*, Nucl. Phys. B **451** (1995) 484 [[hep-lat/9504001](#)].

[118] J. Davies, T. Kaneko, C. Marinissen, T. Ueda, and J. A. M. Vermaseren, *FORM Version 5.0* [[2601.19982](#)].

[119] L. F. Abbott, *The Background Field Method Beyond One Loop*, Nucl. Phys. B **185** (1981) 189.

[120] A. Gynther and M. Vepsäläinen, *Pressure of the standard model at high temperatures*, JHEP **01** (2006) 060 [[hep-ph/0510375](#)].

[121] A. Gynther and M. Vepsäläinen, *Pressure of the standard model near the electroweak phase transition*, JHEP **03** (2006) 011 [[hep-ph/0512177](#)].

[122] A. Ekstedt, P. Schicho, and T. V. I. Tenkanen, *DRalgo: A package for effective field theory approach for thermal phase transitions*, Comput. Phys. Commun. **288** (2023) 108725 [[2205.08815](#)].

[123] L. Born, J. Fuentes-Martín, S. Kvedaraitė, and A. E. Thomsen, *Two-loop running in the bosonic SMEFT using functional methods*, JHEP **05** (2025) 121 [[2410.07320](#)].

[124] L. F. Abbott, *Introduction to the Background Field Method*, Acta Phys. Polon. B **13** (1982) 33.